Development of a sink-source interaction model for the growth of SRC willow and *in silico* exploration of G × E effects

Cerasuolo M[1*], Richter GM[1‡], Richard B[1], Cunniff J[2], Girbau S[2], Shield I[2], Purdy S[3], and Karp A[2]

[1]Sustainable Soils and Grassland Systems Department, Rothamsted Research, Harpenden, Herts AL5 2JQ, UK

[2]Agroecology Department, Rothamsted Research, Harpenden, Herts AL5 2JQ, UK

[3]Institute of Biological Environmental and Rural Sciences (IBERS), Aberystwyth University, Plas Gogerddan, Aberystwyth, Ceredigion SY23 3EE, UK

Running title: Environmental Effects on Willow Genotypes

Highlight:

The process-based model LUCASS gave insights into the sink-source control of willow growth and identified key parameters to predict the performance of perennials in different environments.

Part	Max word number	submission
Abstract	250	218
Total main body + references	10,000	8079
Figures (captions)		8 (357)
Tables		3 (1169)
SI (Model description)		
References		87 (2534words)

‡**Corresponding author:** goetz.richter@rothamsted.ac.uk

Telephone: +44 (0)1582 763 133; Fax +44(0) 1582 760 981

*Current address: Department of Mathematics, University of Portsmouth, Lion Gate Building, Lion Terrace, Portsmouth, Hampshire PO1 3HF, UK

Abstract

Identifying key performance traits is essential for elucidating crop growth processes and breeding. In *Salix* spp. genotypic diversity is being exploited to tailor new varieties to overcome environmental yield constraints. Process-based models can assist these efforts by identifying key parameters of yield formation for different Genotype × Environment combinations. Here, four commercial willow varieties grown in contrasting environments (West and South-East UK) were intensively sampled for growth traits over two 2-year rotations. A sink-source interaction model was developed to parameterise the balance of source (carbon capture/mobilization) and sink formation (morphogenesis, carbon allocation) during growth. Global sensitivity analysis identified day length for the onset of stem elongation as most important for yield formation, followed by various "sink > source" controlling parameters. In coastal climate the chilling control of budburst ranked higher compared to the more eastern climate. Sensitivity to drought, including canopy size and rooting depth, was growth-limiting in the South-East but not in the west of the UK. Light use efficiency increased during perennial maturation of the crop, distinguishing varieties according to canopy size and emphasized quantum efficiency at low light intensity as key to assimilation. However, on average sink parameters were more important than source. The Genotype × Environment pairings described with this new process model helped to identify parameters of sink-source control for future willow breeding.

Keywords: *Salix*; modelling; carbon allocation; sink-source interaction; sensitivity analysis; genotype

Introduction

Yield improvement is an important objective in the development of woody biomass feedstocks from short-rotation coppice (SRC) (Karp and Shield, 2008; Volk *et al.*, 2006). Poplar (*Populus* spp.) and willow (*Salix* spp.) are comparatively young in their domestication (Karp *et al.*, 2011; Stanton *et al.*, 2014) and pedo-climatic adaptation (Aylott *et al.*, 2008; Toillon *et al.*, 2013). However, yields have been doubled by breeders selecting mainly for total biomass, stem traits and disease resistance (Karp *et al.*, 2011). Traits associated with vigour (Kauter *et al.*, 2003; Verlinden *et al.*, 2013; Volk *et al.*, 2006; Weih and Nordh, 2005), development (Toillon *et al.*, 2013; Verwijst *et al.*, 2012), photosynthesis (Andralojc *et al.*, 2014; Robinson *et al.*, 2004) and water use efficiency (Deckmyn *et al.*, 2004; Weih and Nordh, 2002) are now also being incorporated. However, experimental evidence for carbon assimilation (source formation) and its linkage to allocation (sink formation) to above- (AGB) (Bullard *et al.*, 2002b; Guidi *et al.*, 2009; Laureysens *et al.*, 2003) and belowground biomass (BGB) (Heilman *et al.*, 1994; Martin and Stephens, 2006; Matthews, 2001; Pacaldo *et al.*, 2013; Rytter, 2001) has yet to be integrated.

Process-based simulation models are useful tools for integrating knowledge and assessing the relative importance of traits, particularly in woody perennials with long growth cycles, where gathering experimental data is time consuming and expensive (Karp *et al.*, 2014). SRC comprises successive harvest (coppicing) rotations lasting two to three years, where “re-growth” after harvest occurs from basal buds on coppiced stools whilst successive “annual growth” before harvest occurs from buds on the stems. Annual re-growth from reserves was poorly addressed in early models (Le Roux *et al.*, 2001), despite its importance (Ceulemans *et al.*, 1996; Philippot, 1996). The existing models for SRC treat growth either as source-dependent (“top-down”), limited by light interception and use efficiency (Tharakan *et al.*, 2008), or as sink-dependent (“bottom-up”) and influenced by coppice response and carbon allocation (Deckmyn *et al.*, 2004). For phenological development a simple empirical canopy model (Deckmyn *et al.*, 2004) was later replaced by a temperature-controlled budburst model (Deckmyn *et al.*, 2008), and adapted for SRC without validation (Tallis *et al.*, 2013). The need to model temperature control of dormancy, currently debated in many species (Fu *et al.*, 2012), is also unclear in willow (Savage and Cavender-Bares, 2011). Indeed, the whole system of yield formation, dormancy

86 break, budburst and start of photosynthesis needs to be integrated with the initiation
87 of stem growth (sink formation).

88 Carbon allocation and sink formation has often been simplified in previous models
89 (Deckmyn *et al.*, 2004) and allocation to BGB reserves ignored, despite its potential
90 importance for regrowth after coppicing (Ceulemans *et al.*, 1996; Tschaplinski and
91 Blake, 1995). Control of early soft wood production by labile carbon allocated to
92 tree reserves (Deckmyn *et al.*, 2008) has recently been observed for SRC (Verwijst
93 *et al.*, 2012). The importance of reserves for regrowth was also shown in perennial
94 forage crops (Schapendonk *et al.*, 1998; Teixeira *et al.*, 2007). For grassland a sink-
95 source interaction model was proposed (Schapendonk *et al.*, 1998) where assimilate
96 allocation is controlled by sink formation. A similar control has been implemented
97 for carbon partitioning in forest models (Fourcaud *et al.*, 2008; Pretzsch *et al.*, 2008).
98 Carbon translocation is important for both, SRC and grass, which show die-back of
99 stems and tillers, respectively. Data from empirical protocols (stem number, length
100 and diameter), used for SRC phenotyping, can be used for the development of a
101 hybrid model, which combines morphometric data with an eco-physiological process
102 model as suggested by (Pretzsch *et al.*, 2008). This is similar to the approach to
103 predict yields of specific willow clones proposed by (Amichev *et al.*, 2011).

104 To simulate growth processes sufficiently well for use in willow breeding, there is a
105 clear need to derive an integrated model that adequately incorporates key
106 phenological processes and morphogenesis controlling AGB, whilst also taking into
107 account BGB and the influence of reserves. In particular, it is important to integrate
108 new experimental evidence, assess sink- and source-limitations, rank genotype-
109 specific parameters and identify the most important ones to focus breeding efforts.

110 To address these challenges we developed a sink-source interaction model, LUCASS
111 (Light Use and Carbon Allocation in Salix Species) in which phenology controls
112 growth and yield formation. This model describes and predicts the growth of four
113 commercial willow genotypes. The model was calibrated for potential and water-
114 limited production using detailed field data at two different sites in the UK. Key
115 parameters for yield formation, across varieties and in different environments, were
116 identified using a global sensitivity analysis. Finally, the model was validated against
117 independent datasets.

Materials and Methods

Field experiments

Detailed observations describing plant growth were recorded in two identical field trials laid out in a randomised block design consisting of four blocks (Cunniff *et al.*, 2015). Each block contained four commercial *Salix* varieties (Endurance (*S. redheriana x S. dasyclados*), Resolution (multiple parental crosses of *S. viminalis x S. schwerinii*), Terra Nova ((*S. viminalis x triandra*) *x S. miyabeana*) and Tora (*S. schwerinii x* (*S. viminalis* × *viminalis*)) in individual plots of 224 m^2. Details can be found in Table 1 in Cunniff et al. (2015). These varieties were grouped according to phenotype of broad-leaved, closed canopy (Endurance, END; Terra Nova, TN) and narrow-leaved, open canopy (Resolution, RES; Tora, T). The crops were planted in double rows (16,000 cuttings ha^{-1}) in May 2009 and coppiced in January 2010, 2012 and 2014. Destructive and non-destructive measurements of AGB and BGB traits were taken from respective plot areas during two successive 2-year rotations (R1, first rotation, 2010-2011; R2, second rotation, 2012-2013) to populate an extensive database for research and model development.

Locations

The experiments used for model parameterisation (where previous data were not available), calibration and internal evaluation were located in south east England (51.82°N, 0.38°W) at Rothamsted (ROTH) and Aberystwyth (ABER) in Wales (52.4139°N, 4.014°W). Soils were characterised as a silty clay loam (chromic Luvisol) and a shallower sandy silt loam (eutric endoleptic Cambisol), respectively. Final yield data, available for three of the varieties, collected from separate trials at Long Ashton (LARS) in Somerset, England (51.43°N, 2.65°W) and ROTH between 2001 and 2010 were used for external model validation. LARS soil was classified as a coarse loam over clay (stagnogley) to clay (argillic Pelosol), see Table S1.

The long-term averages characterize ROTH as drier with a higher probability of water stress (704 mm, 9.3 °C) than ABER (1038 mm, 9.7 °C). Site-specific hourly weather data were recorded. The 1st rotation (R1, 2010-2011) was drier, 2nd rotation (R2), especially 2012, was wetter than the long-term average (**Figure S1; Table S2**).

Over all years, annual radiation at ROTH was about 20% higher and the temperature range (T_{min}/T_{max}) wider than at ABER (Table 1).

<Table 1>

Phenotyping

Budburst was recorded annually (2010 to 2013), and buds were scored on 10 trees from early February twice weekly until bud swelling then checked daily. Adapting a 7-point scale (Weih, 2009), budburst was defined as green leaf tips (<5mm) visible. Senescence was scored weekly through September to October using 10 trees per treatment and block, adapting a 7-point scale (Fracheboud *et al.*, 2009), defining its onset as >25% yellow/brown and <10% abscised leaves.

Plant architecture (height, stem length and diameter, and number of stems) was assessed on two pairs of trees, randomly chosen from the non-destructive area of each plot. Leaf area indices (LAI) were estimated at ROTH twice monthly using the SunScan Canopy Analysis system (Delta-T Devices Ltd, Cambridge, UK). LUE was estimated from simulated cumulative woody stem biomass and absorbed photosynthetic active radiation (APAR) based on calibrated LAI.

Carbon allocation rates to AGB and BGB components were determined during the first rotation (2010-2012) by destructively sampling two complete trees per plot at key phenological stages (Cunniff *et al.*, 2015). Stool and roots were excavated to a depth of 0.3m, which is likely to represent >90% of the BGB (Pacaldo *et al.*, 2013). Destructive measurements of leaf weight and area were recorded (Cerasuolo *et al.*, 2013). During the second rotation (2012-2013) the number of destructive samples was reduced to twice a year and final yields were assessed after each 2-year coppicing cycle (Cunniff *et al.*, 2015).

Model description

The process-based willow growth model LUCASS (**Figure 1**) simulates development and growth of *Salix* spp., considering phenological (budburst, growth, senescence and dormancy) and morphological plant development (sink formation), and light interception, photosynthesis and respiration (source formation). The AGB and BGB organs (leaves, branches, stems, and stool and roots, respectively) are

considered as sinks and the carbon allocation to these sinks is phenologically controlled and balanced within the sink-source interaction model (Schapendonk *et al.*, 1998). The sinks are phenotypically dimensioned by stem and leaf numbers, their respective elongation rates and specific dry matter densities, which define the carbon demand from a common source pool fuelled by photosynthesis and mobilisable reserves.

<Figure 1>

These processes are controlled by external variables (global radiation, air temperature and water availability), provided by an environmental modelling framework (Richter *et al.*, 2006) that simulates the water and energy balance. LUCASS follows a bottom-up approach where light interception, photosynthesis and respiration (Goudriaan and van Laar, 1994) are simulated with an hourly time step as part of the energy balance. Assimilate allocation to biomass components (leaf, branch, stem, stool and roots) and respective reserve pools are calculated daily. Source-sink carbon flows are considered independently, however, carbon from senescing biomass (leaves, branch die-back) is translocated to the reserves.

Phenology

LUCASS simulates the multi-annual cycle of phenological development at the centre of process control (Figure 1): budburst and leaf emergence, growth of individual organs, senescence and stem die-back, and dormancy to control the onset and duration of carbon capture (source formation) and its allocation to various sinks, as done in grape vine (Vivin *et al.*, 2002).

Budburst, leaf emergence and elongation

Similar to earlier work (Tallis *et al.*, 2013) the budburst was simulated combining a chilling phase followed by a forcing period (Chuine, 2000; Hlaszny *et al.*, 2012). Budburst dates were calculated (eq. S1) using daily mean air temperature (T_{avr}), a half-efficiency temperature (T_C) and a chilling threshold, C_r; both, T_C and C_r, were estimated using genotype-specific budburst data. The other parameters were adapted from (Hlaszny *et al.*, 2012). Chilling unit accumulation started with senescence during the previous season. In keeping with the known biology (Rinne *et al.*, 2011)

208 negative chill units (C_u) accumulate during endo-dormancy until plants reach C_r as in
209 (Cesaraccio *et al.*, 2004). At this point the model plants enter eco-dormancy, an
210 inactive "standby" phase, to accumulate daily forcing (anti-chill) units (C_a), which
211 results in budburst when $C_r + \sum C_a \geq 0$.

212 Leaf emergence rate was calculated as suggested by (Porter *et al.*, 1993) and
213 adjusted by photoperiod, water availability and level of reserves (eq. S2). The leaf
214 emergence declined exponentially over the year. Potential leaf elongation rate was
215 considered dependent on average temperature and day length (Mcdonald and
216 Stadenberg, 1993), modified for plant age (Robinson *et al.*, 2004) and water stress
217 (eq. S3).

218 *Senescence and canopy duration*

219 The model considers leaf senescence as a function of age (accumulated thermal time,
220 μ_T), shading (μ_s, LAI >3) and water stress (μ_w). The start of senescence depends on a
221 threshold day-length, while the date of growth cessation (budset) is modelled as a
222 function of accumulated thermal time; both values were estimated using
223 experimental data (senescence score; end of stem extension) collected at ROTH and
224 ABER during R1.

225 *Stem and woody biomass development*

226 Experimental evidence suggested modelling the onset and rate of stem extension as a
227 function of day length (eq. S5) with a developmental switch considering the base
228 temperature for stem elongation (T_{bStE} =10 °C). This is in contrast to grass models in
229 which leaf and stem extension are determined by temperature (Hoeglind *et al.*, 2005;
230 Schapendonk *et al.*, 1998). The dynamics of stem number is described by a function
231 of the number of initial buds, which form stems and their calibrated die-back rate.
232 The demography of leaves (Porter *et al.*, 1993) and stems (Hoeglind *et al.*, 2005;
233 Schapendonk *et al.*, 1998) was incorporated in order to consider the empirical
234 evidence for re-growth after coppicing, e.g. die-back (self-thinning) of stems. The
235 model does not consider plant mortality (Bullard *et al.*, 2002b).

236 *Sink formation*

237 *Leaf area and biomass*

238 Total leaf area is a function of leaf number, size and shape, scaled to LAI (eq. S4).
239 Initially, willow varieties produce a large number of small shoots in order to rapidly
240 increase leaf area. These branches were treated as "super-leaves" (long leaves whose
241 area is equal to the cumulative area of leaves on the branch), whose growth rate
242 follows the normal-leaf emergence and elongation rate. The leaf area is converted to
243 leaf biomass using a dynamic specific leaf area ($SLA_{min/max}$; (Schapendonk *et al.*,
244 1998)) that accounts for increasing leaf thickness and variable level of reserves. In
245 the model mobilisable leaf carbon is translocated during senescence.

246 *Stem and woody biomass*

247 Potential stem elongation is modelled using a linear function of day length
248 multiplied by a Heaviside function for the effect of daily average air temperature
249 (Powers *et al.*, 2006) (eq. S5).

250 The woody growth potential is expressed in terms of total dry biomass production,
251 which was computed from the average stem volume and specific stem dry weight,
252 multiplied by the observed/simulated number of stems still alive. The stem volume
253 depends on stem length and diameter/height ratio (m_{DH}; eq. S6) modified by a shape
254 parameter η_{St} (eq. S7), as stems are not exact cylinders.

255 *Belowground biomass*

256 The stool and coarse and fine roots are the components of BGB modelled defining
257 respective elongation rates, radial extension and specific densities. Parameters define
258 allocation (de Neergaard *et al.*, 2002) and turnover (Rytter, 2001) rates of fine root
259 dry matter.

260 *Source formation*

261 *Light interception*

262 The genotype specific light interception is described by a pseudo-3D architectural
263 model (Cerasuolo *et al.*, 2013), which defines horizontal and vertical spatial

distribution of leaves in a gap fraction model, characterising LAI by clumping (Ω) and profile shape (η) factors. The LAI is computed daily and the cumulative LAI is considered as $\Omega \times L_c(z)$, where $L_c(z)$ is the distribution of leaf area over the canopy depth (z). The light interception module describes the effect of canopy clumping on both, direct and diffuse radiation (De Pury and Farquhar, 1997). The extinction coefficient for the diffuse radiation is calculated according to (Goudriaan, 1988), with weighted contributions from the three zones of a standard overcast sky. To simulate light interception the canopy is divided into five layers, which are either uniformly or asymmetrically distributed. Within each layer the ratio of sunlit/shaded leaf area is calculated to estimate the vertical variation of photosynthesis inside the canopy.

Photosynthesis and carbon pools

Photosynthesis is computed as the assimilation rate of carbon dioxide (CO_2) using the maximum between an exponential function of the intercepted energy (absorbed photosynthetic active radiation; APAR) and its potential absorption, modified by CO_2 air concentration and air temperature (Goudriaan and van Laar, 1994). The effect of soil water availability on stomatal conductance and reduction in CO_2 absorption is represented using a logistic function to describe the reduction of photosynthesis with decreasing relative soil water content (Sinclair, 1986).

Three different biochemical pools are simulated: First, a source pool of available carbohydrates (C_{av}) composed of photosynthetic assimilates and remobilised reserves used for growth and maintenance processes. Second, a source/sink pool of mobilisable carbohydrate reserves (e.g. starch) in leaves, wood and stool. Finally, the sink pool of structural biomass, divided into *AGB* (stems, branches and leaves) and *BGB* (stool, coarse and fine roots).

Sink-source interaction

Carbon allocation

The allocation of C_{av} is modelled as a combination of a sink-source balance and a hierarchical cascade (leaf > stem ≈ [stool & root]). The respective sink strengths result from genetically determined growth potentials (see above) defined by the

maximum rate of each organ's dry matter accumulation and turnover (Genard *et al.*, 2008).

The total source (C_{av}; eq. 1a) to satisfy sink demands is calculated as the net daily integral of the difference between hourly leaf photosynthesis (CH_2O) and maintenance respiration of the respective tree organs ($R_{t;}$ eq. 1b), plus the mobilisable reserves from leaves (Lf_{Res}), woody biomass (W_{Res}), and stool (Stl_{Res}):

$$C_{av} = CH_2O - R_t + Lf_{\mathrm{Res}} + W_{\mathrm{Res}} + \alpha \times Stl_{\mathrm{Res}}, \quad (1a)$$

$$R_t = \left(m_{Lf} \times Lf + m_B \times B + m_{Stl} \times Stl\right) \times Q_{10}^{\frac{T_{avr} - T_{Q10}}{10}} \quad (1b)$$

A fraction of Stl_{Res} (α = 0.04) can be mobilised for 20 days after budburst ((Deckmyn *et al.*, 2008) ANAFORE Manual). If new assimilates exceed sink demands (Schapendonk *et al.*, 1998) the emerging surplus of assimilates is allocated to the reserve pools. The available carbohydrates for aboveground biomass (AGB_{av}) are converted into leaf (*LfB*) and woody stem biomass (*WSB*) using their respective conversion factors (Penning de Vries *et al.*, 1983) and potential sink increases:

$$LfB = AGB_{av} \times LfGrPt / ShGrPt, \quad (2a)$$

$$WSB = AGB_{av} \times SGrPt / ShGrPt. \quad (2b)$$

Here *ShGrPt* represents the total shoot growth potential, and *LGrPt* and *SGrPt* the leaf and stem growth potentials, respectively.

C_{av} is partitioned between AGB_{av} and BGB_{av} using constant potential allocation coefficients, derived from the experimental evidence. These allocation coefficients change with stool size to account for increasing plant vigour during establishment and drought to increase root growth for better resource capture (Goudriaan and van Laar, 1994).

$$StlB = BGB_{av} \; x \; StlGrPt/BGGrPt \quad (3a)$$

$$RtB = BGB_{av} \; x \; RtGrPt/BGGrPt \quad (3b)$$

Stool and roots are assumed to turnover with different rates; stools are set to have a longevity, which corresponds to the stand/plant life-time (Bullard *et al.*, 2002b), whilst fine roots are set to a high annual turnover rate (Rytter, 2001).

Consecutively, C_{av} is allocated to the plant organs according to their respective sink strengths, defined by LAI and SLA, wood volume and density, stool mass, root growth and turnover. Daily carbon allocation is, therefore, either limited by C_{av}, or by the effective sink demand of assimilates (potential growth). At each time step, LUCASS balances the gain and consumption of carbon, estimates the conversion of C_{av} into growth, and calculates the produced biomass (g m^{-2} upscaled to kg ha^{-1}).

Effects of the environment

The soil hydrology is modelled using an energy balance approach combined with a two layer soil water module (Richter *et al.*, 2006). The energy fluxes at the canopy surface are controlled by crop characteristics (LAI, stomatal resistance, canopy height), climatic variables, and soil hydraulic properties (Table s1). The rooting depth is dynamic and calculated using a constant crop specific root advancement coefficient and a maximum rooting depth. The soil water balance, transpiration and water uptake, are calculated using the Penman-Monteith equation. The plant water stress variable, k_{WS}, is described by a non-linear, logistic function (eq. S2c) in dependence of the relative water content between minimum and maximum plant available soil water (Sinclair, 1986). Its curvature is determined by the water stress parameter, *WSP* (Table 2), which was calibrated using R1 data at ROTH. A/BGB partitioning is modified according to soil water availability (van Laar *et al.*, 1992).

<Table 2>

The effects of water stress on leaf emergence and elongation rates, and stem and leaf mortality are also considered as a function of k_{WS} and respective potential rates. Buds and branches follow the same dynamics as leaves, but the mortality rate of branches is assumed to be 10 times lower than that of leaves. The mortality rate of stems is also computed as the sum of natural turnover and death rate caused by water and shading stress, however, stem mortality is less than that of leaves (**Table S2**).

Calibration and parameter ranking

The model inputs divide into environmental variables and process parameters: (i) field location (longitude, latitude etc.) and soil characteristics; (ii) management data (irrigation, harvest days, number of years per growth-cycle); (iii) [hourly] weather

data, e.g. solar radiation, mean air temperature, wind speed and direction, rainfall and air humidity; and (iv) genotype-specific growth parameters.

Model calibration

The parameters of the growth model were calibrated using genotype-specific experimental data where values from the literature were not available (**Table 2**). Process-specific evidence was used to calibrate development and morphology either through direct measurements (e.g leaf emergence and senescence) or through parameter estimation involving model data fitting (e.g. budburst, stem height and stem diameter). Model cross-validation was performed using time-series of the variables not used for calibration (e.g. canopy height, stem biomass). The photosynthesis parameters (Bonneau, 2004) were calibrated to match total biomass production and turnover.

Parameters of the budburst model (eq. S1) were calibrated using ROTH data from the first rotation cycle (2010-11), while parameters for stem height/diameter relationships were estimated using data from both locations (ABER and ROTH, 2010-11). LUCASS (remaining parameters) was calibrated for potential productivity using data from ABER assuming that water was unlikely to limit growth and carbon partitioning. The flux parameters for carbon allocation were calibrated using morphological components of AGB (leaf and stem weight) and BGB (stool and fine root weight). In a final step, water stress effect on biomass production was calibrated using time series of data collected at ROTH (e.g., LAI).

Sensitivity analysis

A global sensitivity analysis (SA) was performed for all varieties and both sites for potential (no water stress, NWS) and actual (water stress, WS) growth, and the model response was determined for the first and second coppice rotation (R1, R2). The aim was to understand which growth parameters had a significant impact on final yield, whether it changed with the environment, age of stand or phenotype. All of 78 parameters (Table 2) were varied in a one-at-a-time modus using the Morris' method (Morris, 1991). Assuming that all parameters were normally distributed (Richter *et al.*, 2010) the window of their variation was set to a respective standard deviation of 10%. The estimated average response strength (μ) for each parameter

represents its overall effect on the model outcome (e.g. final yield). Its standard deviation (σ) represents the response spread estimating higher order effects (non-linearity, parameter interactions). Both μ and σ were calculated over six different trajectories (individual one-parameter-at-a-time simulations) and using six levels (granularity of the explored parameter space) (Richter *et al.*, 2010).

Data analysis and model validation

Data were analysed with Genstat^{TM} 14 (Payne *et al.*, 2011) to examine the influence of location and varieties using a two way Analysis of Variance (ANOVA). Linear regressions were performed using Sigmaplot (version 12.0, 2011). The model was validated against yield data from the second growth cycle at ROTH, and independent datasets for three of the four varieties at LARS and ROTH. The goodness of simulations to match experimental data for the two dedicated trials was characterised with the Residual Mean Square Error (RMSE). The coefficient of determination, the model efficiency (ME), RMSE, bias (Mean difference, MD) and r^2 were calculated according to (Smith *et al.*, 1997).

Results

All following results fall into a distinct pattern due to significantly different climatic conditions during the two rotations where R1 was distinctly drier than R2, which translated into high water stress, especially in 2010, and low water stress, especially in 2012. These conditions were exacerbated by site differences and reached almost potential (NWS) conditions in ABER during 2012 whilst ROTH had strong WS conditions during R1 growth.

Sensitivity analysis

Identification and ranking of key parameters

The heat map details (**Figure S2**) showed a clear pattern of high sensitivity under potential (NWS) and low water stress (R2) growing conditions which translated clearly into the aggregated averages (Figure 2). Considering a model response threshold of about 1000 kg ha^{-1} per 10% parameter change (4 to 5% yield potential), the SA revealed that yields were affected by up to 20 parameters (under NWS). Under conditions of growth-limiting WS the number of parameters with significant

413 effects on yield dropped to less than 10. However, these ranked consistently high
414 when considering the average response to their variation across sites (ABER,
415 ROTH), age (R1, 2) and canopy phenotype. Model sensitivity was higher in the
416 second (R2) than in the first rotation (Figure 3) most likely due to lower water stress.
417 Differences between sites were overall small and affected only few parameters (day
418 length associated with buds turning into branches dl_{BtoBr}; A/BG partitioning, ρ_{AB}, and
419 quantum efficiency, φ_{pot}). Most of these parameters reflected experimental evidence
420 and measurable crop traits defining sinks and sources.

421 <**Figure 2**>

422 *Sink formation – Pheno-morphology*

423 The onset of stem elongation (dl_{0SER}) was identified as the overall most important
424 yield determining (phenological) parameter at both sites and for all conditions. It was
425 followed by closely related morphological sink determinants, like stem elongation
426 rate (m_{SER}) and diameter/height coefficient (m_{DH}). The fraction of total biomass
427 allocated to AGB (ρ_{AG}) also ranked among the strongest effects, emphasizing the
428 importance of A/BGB partitioning. The fraction allocated to roots (ρ_{Rt}) had an
429 equally large effect (0.7 to 2.3 Mg ha^{-1}). These sink parameters had a most stable
430 ranking across most of the subsets of the SA; exceptions were rank changes for ρ_{AG}
431 with site and phenotype.

432 Phenological parameters that determine budburst (chilling requirement C_r; base
433 temperature T_c) showed a very inconsistent and contrasting behaviour. C_r ranked
434 overall higher for potential than water-limited growth which was also reflected in its
435 higher rank in the wet second rotation. Differences between sites were marginal but
436 both parameters were slightly more important for ABER than ROTH (**Table S4**);
437 however, C_r ranked on average slightly higher for the open canopy phenotype
438 (Figure 2).

439 *Source formation*

440 Source-related parameters (light interception, photosynthesis) were on average less
441 sensitive than sink-related parameters. Parameters of canopy structure (Ω; η) were
442 identified as important under potential (2.3 and 1.6 Mg ha^{-1}), but not under water-
443 limited production (<0.5 Mg ha^{-1}). On the other hand, parameters determining light

interception, e.g. number of leaves and leaf elongation rate (> 2 Mg ha^{-1}) ranked consistently high, irrespective of the site, rotation or phenotype. The sensitivity of photosynthesis, quantum efficiency, φ_{pot}, was on average more than twice that of A_{max}, emphasizing light conversion at low light levels to be crucial for willow production in the UK. There was a difference between sites (see below) and phenotypes; the change of φ_{pot} was more important in large, closed canopy phenotypes (END &TN).

< Figure 3>

Environmental effects

The overall parameter effects on yield were only marginally higher at ROTH than ABER (0.73 and 0.81 Mg ha-1; Figure 3), but model sensitivity was higher in R2 than R1, which reflected the wetter growth conditions in R2, whilst R1 was characterised by water stress aggravated by higher cumulative radiation (**Table 1**). The relative sensitivity to changes of physiological parameters (photosynthesis) was similar for both sites when tested for potential production (NWS; Table S4). The effects of water stress reduced the overall sensitivity to changes of other physiological parameters (light interception and photosynthesis).

The SA revealed interactions between process and site, e.g. resulting in different parameter rankings related to temperature (budburst and senescence, μ_T) and water, both marginally more important at ROTH than ABER. The high ranking of *WSP* did not translate into similar differences caused by variation of water stress induced senescence, μ_{WS} (**Figure 2**). At ROTH the average effect of source related parameters on yield, like light interception (onset of branching, dl_{BtoBr}, number of leaves per branch, NL_{Br}; Ω; η) and photosynthesis (φ and A_{max}) ranked lower than at ABER, which could reflect an interaction of light (lower radiation) and water availability. In contrast, parameters related to carbon allocation (sink size) ranked higher at ROTH than at ABER.

Model calibration and cross-validation

Phenology, light interception and LUE

Budburst parameter values showed a small variation among varieties (Table S3) with an average value of 6.1 ±0.5 °C and -18.1 ±0.4 for T_C and C_r, respectively. The model explained an overall 79% of the variance in budburst date at ABER. In 2013 budburst showed a reduced goodness of fit by more than 10% at both sites as temperatures were outside the range of calibration.

Light interception is the result of a complex process of leaf area formation (eq. S2-4). Leaf area was first calibrated at ABER using only destructive LAI measurements, and then re-calibrated for water stress against the experimental evidence of LAI at ROTH during the first rotation (**Figure 4 C/F**).

<Figure 4>

The LAI simulation at ROTH (Endurance and Tora in **Figure 4A/F,** and Resolution and Terra Nova in **Figure S3**) was better during the first rotation than during the second (respective RMSE for Endurance were 0.95 and 1.78, Table 3). This was mainly due to delayed canopy development after coppicing in January 2012. Overall, the model reflected the genotypic differences between canopy types quite well but described LAI better for non-coppiced than coppiced years (RMSE of 0.76 and 1.26, respectively).

The parameters for photosynthesis were estimated against total biomass (e.g. **Figure 4** D+E + fine roots), and A_{max} in the range of 18.9 to 23.3 μmol m^2 s^{-1} matched the sink demand well. For Terra Nova we calibrated a value similar to Endurance as both had a similar canopy. For comparison, photosynthesis was also expressed in terms of LUE, based on annual woody AGB (stem yield) and simulated intercepted PAR (**Figure 5A**) and averaged over all years (**Figure 5B**). LUE was 6% lower during 1st compared to 2nd rotation at ROTH but not at ABER. Overall, LUE at ROTH was lower than at ABER, mainly due to 2011, when Tora and Endurance suffered strong reductions (26 and 30%) due to drought.

<Figure 5>

Sink formation – carbon allocation

Potential stem elongation rates were initially calibrated using stem-height data during 2012 at ABER to avoid bias due to carbohydrate limitations and water stress. The parameter values for stem elongation (eq. S5) were then optimised through iteration using ABER genotype-specific growth data (time series) during the 1st rotation (2010-2011). These parameters fitted well the heights observed at ROTH (**Table 3**). The agreement between computed and observed stem extension rates is reflected in the stem growth dynamics at ROTH, in particular for the variety Tora (**Figure 4G**).

Stem number was strongly affected by the environment, with numbers significantly smaller at ABER than ROTH ($p<0.01$) during 2010-2011, and genotype ($p<0.001$) with Endurance having most and Resolution least. A significant interaction between sites and varieties ($p<0.01$) was related to greater range in stem numbers among varieties at ROTH compared to ABER.

The relationship between stem height and diameter also showed a strong interaction between sites and varieties (Figure 5; $p<0.001$). Data showed two separate groups, one for ROTH where stems are thinner and the other for ABER where stems are thicker, for an equivalent height. The parameters m_{DH} and c_{DH} were evaluated for each variety at each site from first rotation data (**Table S5**).

<Figure 6>

Destructive harvest data from both sites (first rotation) were used to approximate the partitioning between AGB and BGB in all varieties (e.g. Figure 4D, E; I, J; see also Figure S3 N,O; S,T). The four varieties allocated between 80% (Endurance) and 90% (Resolution) of the dry matter to the AGB. Stem and stool biomass data at the end of rotations showed that all varieties allocated a smaller fraction of assimilates to BGB during R2 compared to R1. For Endurance it dropped from 20 to 15%, whilst Tora reduced allocation from 15.4 to 11.3%.

Model Validation

Validation using the variety trial at ROTH

The model validation was firstly done by comparing the average LAI, stem height and number, and AGB/ BGB yields measured in the second rotation of growth (R2)

at the dedicated variety trial at ROTH with the corresponding simulations (Table 3). The model predicted the differences in LAI between varieties well, with values for Endurance being highest and lowest for Tora (**Figure 4**). However, LAI modelling efficiency was low due to a phase shift of re-growth during the first year of the second rotation. Separating coppicing from non-coppicing years improved the statistical indicators of the prediction of LAI data (RMSE = 0.76; MD = -0.23; R^2 = 0.61).

<Table 3>

A management × site effect was observed in terms of different stem numbers, height/diameter ratio between ABER versus ROTH across all four varieties (Fig 5). These observations suggested site-specific parameter values for A/BGB partitioning and initial stem numbers and height/thickness m_{DH}.

The final yield predictions agreed in a satisfactory way with the empirical data at ROTH for all four willow varieties for both rotations (R1, cross-validation; and R2, validation) (**Figure 6**). This result is consistent with the fact that for all the varieties we observed a high model efficiency and r^2 (>0.85, Table 3) for stem biomass. The daily simulations for LAI, stem height and biomass, as well as stem number were within the 95% confidence interval of mean observations of these variables (**Figure 4**). The model was able to catch the behaviour of the studied traits throughout the growing seasons for all studied willow varieties. The comparison between measured and simulated BGB was satisfactory for most varieties (Figure 4E/J). ME was high for canopy height (all>0.9) and stem biomass yield (overall due to small number of samples ~0.99), and acceptable for BGB (overall ~0.28) whilst it was low for LAI and stem number (**Table** 3), due to slight asynchronies (**Figure 4**).

<Figure 7>

It is interesting to observe that in wet years [2012 (**Table S2**)] broadleaved varieties (e.g. Endurance, Figure 4D) performed better than the others (e.g. Tora, **Figure 4I**) but were more sensitive to water stress in 2010. The narrow leaf variety Resolution performed well in both rotations, irrespective of water stress (**Figure S3**), displaying an overall interesting G × E interaction. During the second rotation final yields in all varieties were significantly lower at ABER than ROTH. However, ABER second

562 rotation data could not be used for validation as the crop suffered exceptional wind
563 damage that the model could not account for. Significant differences between
564 genotypes ($p<0.001$) established Endurance as the best yielder in both locations.

565 *Validation with further yield data*

566 Simulated and measured final biomass yields for three varieties compared well at
567 ROTH and LARS (**Figure 8**). The overall correlation between measured and
568 simulated biomass yields across both locations was good ($r^2=0.80$) and the average
569 difference small and ME high (MD=0.68 Mg ha^{-1}; ME=0.7). Most of the predictions
570 concentrated near the 1:1-line, proving that the model was able to reproduce actual
571 yields. It showed a slight bias toward lower yields at LARS and overestimated yields
572 at ROTH.
573 **<Figure 8>**

574 ## Discussion

575 The process-based model LUCASS characterized phenotypic carbon sinks and
576 implemented a sink-source interaction to describe yield formation for different SRC-
577 willow genotypes. The novelty of this approach lies in its simplicity to parameterize
578 the size of various sinks using phenotype-specific morphological characteristics.
579 Calibrated and validated with data from sites across the UK, the model was able to
580 illustrate the underlying system behavior in terms of source and sink dynamics and
581 predicted final yields reflecting genotypic and environmental differences.

582 ### Key productivity parameters

583 Compared to other models (Amichev *et al.*, 2011; Deckmyn *et al.*, 2008; Tallis *et al.*,
584 2013) LUCASS has fewer parameters and less than 20 proved to be crucial for yield
585 formation (**Figure 2**). The sensitivity analysis identified the onset of stem
586 elongation, stem elongation rate and diameter as key parameters for yield formation
587 and indicators of vigor (Kauter *et al.*, 2003; Volk *et al.*, 2006). Parameters of early
588 development, e.g. chilling and forcing functions (Cesaraccio *et al.*, 2004; Fu *et al.*,
589 2013) were confirmed to be important at sites with a mild winter climate (ABER,
590 LARS). Despite the importance of the start of spring growth (Cannell and Smith,
591 1983; Weih, 2009), it is not entirely clear whether chilling has a physiological role

(Horvath *et al.*, 2003; Rohde and Bhalerao, 2007) in addition to cold hardiness (Morin *et al.*, 2007). Further investigation is needed to determine whether chilling should be modelled for temperate tree species (Fu *et al.*, 2012). The role of photoperiod (Fu *et al.*, 2012) needs testing over a range of latitudes as sites studied here were similar. Nevertheless, this study did show that photoperiod was important for canopy development in terms of branching (dl_{BtoBr}) and stem elongation (dl_{0SER}).

This analysis also showed that early budburst does not necessarily mean faster canopy development. Despite initial delays after coppicing, e.g. 2012, modelled and observed LAI reached their maxima at similar time and values, and the disparity had no impact on biomass production. A late spring start was apparently compensated for by faster leaf growth when environmental conditions became favorable (Weih, 2009). Thus, although budburst date is important for modelling willow development (Savage and Cavender-Bares, 2011), it remains debatable whether its accuracy is also important for predicting yield (Tallis *et al.*, 2013).

Genotypic differences for routes to high yields?

Source formation:

The variation of willow yield proved highly sensitive to parameters of LAI distribution and genotypic canopy characteristics, confirming that stem dynamics and biomass yield are strongly influenced by radiation distribution within the canopy (Bullard *et al.*, 2002a; Cerasuolo *et al.*, 2013; Ceulemans *et al.*, 1996; Tharakan *et al.*, 2008). Photosynthesis parameters (A_{max}, φ_{pot}) differed across genotypes (Andralojc *et al.*, 2014; Bonneau, 2004) and were also confirmed as an important source of yield variation (**Figures 2 and 3**). Quantum efficiency, φ_{pot}, consistently caused a larger model response than A_{max}, however, both seem to be strongly related, as found by (Andralojc *et al.*, 2014; Kaipiainen, 2009). Genotype ranking, according to photosynthetic capacity at the plant level, was dominated by leaf area but genotypes realized similar biomass with different strategies, either through high photosynthetic rate or large leaf area, confirming previous results (Andralojc *et al.*, 2014).

LUE is a key physiological indicator, usually expressed in terms of woody AGB per

622 unit absorbed PAR, which ranged from 0.6 g m^{-2} MJ^{-1} to 1.7 g m^{-2} MJ^{-1} (**Figure 6A**).
623 Mean LUE was significantly higher at ABER (**Figure 6B**) indicating its interaction
624 with drought and senescence (Savage *et al.*, 2009), canopy duration and leaf
625 abscission (Weih, 2009) which can affect cumulative photosynthesis (Philippot,
626 1996). These site-specific differences due to water stress varied between broad- and
627 narrow leaved varieties (Endurance and Tora, respectively). Tora evaded drought by
628 means of a smaller leaf number (Cerasuolo *et al.*, 2013) and LAI (**Figure 4F**). The
629 lowest LUE values were calculated for the first year of regrowth after establishment
630 (2010), which was aggravated by drought at ROTH, especially for Endurance with
631 its large canopy (-41%). *In situ* measurements under controlled water supply showed
632 a similar drop in photosynthetic efficiency (-33 to -60%; (Bonneau, 2004)). The
633 range of average LUE (0.77 to 1.47 g MJ^{-1}) which was significantly different
634 between sites ($p<0.01$) and varieties ($p<0.001$) agreed with the range of simulated
635 values (Jing *et al.*, 2012) and other estimates (Bullard *et al.*, 2002a; Sannervik *et al.*,
636 2006; Tallis *et al.*, 2013). A large canopy increased a variety's sensitivity to water
637 stress, e.g. lowest LUE of Endurance irrespective of location, but achieved high
638 yields in wet conditions. The effects of senescence on nutrient remobilization
639 (Fracheboud *et al.*, 2009) and dry matter loss through respiration (de Neergaard *et*
640 *al.*, 2002) can complicate the G × E interaction under variable climate.

641 *Sink formation*

642 Morphological characteristics were most important to identify high yielding
643 genotypes especially under water stress conditions. The high sensitivity of these sink
644 parameters across both sites (**Figure 2 and 3**) confirmed their importance for yield
645 formation (Larsson, 1998). Traits, like stem number, height and diameter as well as
646 leaf size and form, are also easily measured in high-throughput screening (Bullard *et*
647 *al.*, 2002b; Martin and Stephens, 2006; Sannervik *et al.*, 2006; Sennerby-Forsse and
648 Zsuffa, 1995; Verwijst *et al.*, 2012).

649 Our results confirmed earlier findings that Endurance had the thickest stems whilst
650 Resolution the thinnest (Cunniff *et al.*, 2011). The genotype-specific relationship
651 between stem diameter and height (**Figure 5**) is an excellent example of integrating
652 plant characteristics and environment influence (G × E interaction). Stem diameter
653 increases with length of coppicing cycle and is an important determinant for wood

quality (bark fraction) (Guidi *et al.*, 2009; Kauter *et al.*, 2003) and harvestable wood volume (Amichev *et al.*, 2011; Bullard *et al.*, 2002b).

Moreover, parameter values for the potential allocated AGB were considered ~10-12% lower than those estimated from destructive measurements. This was due to the concurrence of two factors: around 30-40% of the NPP produced by basket willow was used belowground, in particular on fine roots due to their high turnover rate (Rytter, 2001). Experimental evidence provided by soil cores collected at ROTH showed that actual fine root biomass was three times that from destructive samples, e.g. Endurance 873 versus 283 g/m^3, respectively (Cunniff *et al.*, 2015). These root cores also showed that willows had a 65% greater fine root volume when grown at ABER compared to ROTH.

The analysis of the experiments showed differences in carbon storage in BGB (Cunniff *et al.*, 2015), which could have affected the regrowth dynamics (Sennerby-Forsse and Zsuffa, 1995; Tharakan *et al.*, 2008; Verwijst *et al.*, 2012). Poor yields of Tora under drought were shown to be concurrent with low initial BGB. Root biomass could be a key trait to mitigate such circumstances (Ceulemans *et al.*, 1996). Tora showed great resilience to yield high in the second growth cycle by building up comparable fine root mass (Cunniff *et al.*, 2015). However, the G × E interaction is not conclusive: in spite of more investment of carbon in BGB at ABER the vigour after coppicing in 2012 dropped considerably (Cunniff *et al.*, 2015). Experimental data also showed significant differences in biomass allocation among varieties ($p<0.001$) and in the interaction between site and variety ($p<0.05$) (Cunniff *et al.*, 2015; Cunniff *et al.*, 2011). Stem numbers were possibly related to soluble sugars/starch availability; but difficult to separate from management effects (cut-back) at ABER which resulted in a smaller stool volume with fewer buds to develop into new stems (Cunniff *et al.*, 2014).

Further analyses of the underlying physiological processes are needed to justify different modelling approaches for early development (Fu *et al.*, 2012) and impact on early growth (Tharakan *et al.*, 2008; Verwijst *et al.*, 2012) and yield formation. A systematic budburst delay after coppicing can be expected (Verwijst *et al.*, 2012). Bud and stem numbers could be influenced by stool size (management effect) as well as starch and sugar contents (Cunniff *et al.*, 2014; Tschaplinski and Blake,

686 1995). This and evidence in regard to regrowth after coppicing (Tschaplinski and
687 Blake, 1994; Von Fircks and Sennerby-Forsse, 1998) suggests model expansion to
688 describe number of buds bursting as a function of readily available carbohydrate.

689 BGB characterization within the system is essential (Karp and Shield, 2008) but few
690 data exist for roots of SRC (Agostini *et al.*, 2015; Cunniff *et al.*, 2015; Pacaldo *et al.*,
691 2013; Rytter, 2001). Destructive harvests represented only part of the belowground
692 allocation (20 and 10% of the total measured biomass). A similar amount of fine root
693 mass in a 1-m profile (3.56 and 6.46 Mg ha^{-1}) can be added (Cunniff *et al.*, 2015),
694 which usually turns over fast (Rytter, 2001).

695 *Source –sink interactions under different environments*

696 Within the sink-source interaction the LAI and stem growth play the key roles for
697 potential production, balancing the available CHO for resource capture and
698 harvestable biomass. A hierarchy of dry matter allocation to leaves over stems was
699 needed to enable sufficient light capture. In the model LAI is influenced by budburst
700 and base temperature for leaf growth, which usually precede the day length threshold
701 for stem elongation. Sufficient allocation of CHO to leaves (and fine roots) was
702 secured by considering a genotype-specific T_{base} for stem elongation in the range of 8
703 to 10°C independent of location. These experimentally founded values are much
704 higher than those suggested for the variety Jorr (2 to 7.6 °C) (Martin and Stephens,
705 2008). The discrepancy between T_{base} values for shoot extension is probably due to a
706 different interpretation of this parameter. In contrast to T_{base} within a linear function
707 of stem elongation rate and air temperature (Martin and Stephens, 2008) LUCASS
708 used T_{base} to switch carbon allocation from “leaves only” to “leaves + stems”, stem
709 elongation mainly depending on day length.

710 LAI between 2 and 4 were sufficient to reach high biomass yield (Jing *et al.*, 2012),
711 suggesting that with the exception of Endurance, all varieties were source limited
712 during the first year of regrowth (**Figure 4 and S3**). As LUCASS simulated seasonal
713 dynamics of CHO reserves explicitly reserve pools balanced seasonal fluctuations in
714 carbon availability. Overall, the agreement between measured and modelled sink
715 indicators was good across the validation datasets (**Table 3**), even for stem numbers,
716 although the dynamic of stem numbers was less well represented (**Figure 4**).

717 According to our simulations the stem as the major sink accounted for 75 to 97% of
718 the yield variance, variation of stool weights (**Figure 4**; 47 to 95%), and plausible
719 values for root dry matter. Furthermore, 94 and 80% of the yield variance was
720 captured across cross-validation at ROTH and independent data sets (LARS,
721 ROTH), respectively.

722 The necessity to define site specific initial bud and stem numbers to compensate for
723 environmental and management (coppicing) effects shows the need for a more
724 mechanistic description of coppicing response. Stored carbohydrates in the reserve
725 pools are essential for the initial growth of perennials (Philippot, 1996), and the
726 available evidence (Cunniff *et al.*, 2015; Cunniff *et al.*, 2014) would allow
727 implementation of a functional relationship between reserve availability and
728 stem/bud numbers to describe regrowth (Bullard *et al.*, 2002b; Tharakan *et al.*,
729 2008).

730 Allocation to BGB was a limiting factor for development of AGB during crop
731 establishment and can be considered as one cause for low yield during the first
732 rotation. Water limitation caused further significant reduction of AGB in favour of
733 BGB at ROTH, and LUCASS simulated both limitations adequately. The varieties
734 showed different responses towards water stress from a very sensitive Endurance to
735 an almost tolerant Resolution (Bonneau, 2004; Larsen *et al.*, 2014; Savage and
736 Cavender-Bares, 2011). New evidence from specific experiments with potential-
737 and limited-water treatments will follow in future.

738 In conclusion, this model represents a valuable research tool to improve selection
739 and breeding programs for site-specific SRC crops in support of the “fuel versus
740 food” debate and to explore climate and land use scenarios for the development of
741 biomass resources needed for the bioeconomy. LUCASS’ ability to simulate
742 allocation to BGB also allows improvement of the terrestrial carbon balance and soil
743 carbon sequestration to be assessed.
744

Supplementary data

Model equations S1 to S7

Supplementary Figures

Figure S1: Global solar radiation (- -), air temperature (—) and precipitation (filled bar) at Rothamsted (a) and Aberystwyth (b) during the experiment (2010-13)

Figure S2: Heat map from sensitivity analysis displaying the average response strength (μ) estimated using the Morris' method, run for all varieties at both sites, Harpenden (ROTH) and Aberystwyth (ABER) with weather data for first (R1, 2010-11) and second rotation (R2, 2012-13). Simulations were done in absence of water stress (NWS) and under actual water stress (WS).

Figure S3: Observed (filled circles) and simulated (solid line) leaf area index (LAI), canopy height, stem number and accumulated stem (AGB) and stool (BGB) biomass of Resolution (K-O) and Terra Nova (P-T) grown at Rothamsted over two consecutive 2-year rotations (2010-11; 2012-13). The error bars represent the standard deviations of the experimental values (n=4)

Supplementary Tables

Table S1: Physical characteristics of the soil in three sites using Soil Classification System for England and Wales: Harpenden (ROTH), Aberystwyth (ABER) and Long Ashton Research Station (LARS); soil depth, bulk density, soil texture (sand, silt and clay), soil organic carbon (SOC), volumetric water content at field capacity θ_{fc} and permanent wilting point θ_{pwp}, available water capacity (AWC) in the profile derived using the Hypres pedotransfer function (Wösten *et al*., 1999).

Table S2 Cumulative annual precipitation, radiation, and average minimum and maximum temperature (2010-2013) and the two sites (ROTH and ABER)

Table S3: Optimised values of the parameters T_C and C_r of the chilling model (1) for each willow variety.

Table S4: Results of the sensitivity analysis for ROTH and ABER simulated under potential (NWS) and water-limited (WS) production for (a) the first (2010-11) and (b) the second coppice rotation (2012-13).

774 Table S5: Parameter values for the stem height/diameter relationship, for the
775 four studied varieties (Endurance, Resolution, Terra Nova and Tora) and the two
776 dedicated trials (ROTH and ABER).

777 **Acknowledgments**

778 The authors would like to thank the Biotechnological and Biological Sciences
779 Research Council (BBSRC) and Ceres Inc. for funding this work within the
780 "BBSRC Sustainable Bioenergy Centre (BSBEC): Perennial Bioenergy Crops
781 Programme" (BB/G016216/1; http://www.bsbec-biomass.org.uk/). We would also like
782 to thank Tim Barraclough, March Castle, William Macalpine and Peter Fruen
783 (Rothamsted), and Anne Maddison and Laurence Jones (Aberystwyth) for their
784 dedicated work collecting data in the field.
785

Tables

Table 1: Meteorological indicators during dormancy (November – March) and growth (April – October) periods mean maximal and minimal air temperature (T_{max}, T_{min}) and cumulative annual global radiation (R_g) and precipitation (P).

	Dormancy		**Growth**			
	T_{max}	**T_{min}**	**T_{max}**	**T_{min}**	**R_g**	**P**
Site	**(°C)**				(MJ m^{-2})	(mm)
ROTH	7.6	1.8	17.7	9.0	3910	680
ABER	9.0	3.8	16.6	11.6	3560	1020
LARS	9.2	3.1	18.5	10.4	3740	760

Table 2: Alphabetical list according to process of model parameters used in LUCASS; symbols, definition and units as well as source (reference, experimental evidence)

Symbol	Definition	Units	Reference/Comments
Phenology			
C_r	*Chilling requirement*	d	Optimised
d_{ac}	*Number of day necessary to the crop to reallocate resources*	d	Optimised
dd_{fill}	*GDD for max stem filling rate*	°C d	Calibrated
dl_{0SER}	*Stem elongation rate, intersect*	d	Measured
dl_{BtoBr}	*Base photoperiod of buds becoming branches*	d d^{-1}	Assumed
$dl_{maxBtoBr}$	*Photoperiod for maximum rate of buds becoming branches*	d d^{-1}	Assumed
$NBuds_0$	*Initial bud number*	-	Measured
T_B	*Base temperature for above ground growth*	°C	(Perttu and Philippot, 1996)
T_c	*half-efficiency temperature*	°C	Optimised
$T_{optBtoBr}$	*Optimum temperature for buds becoming branches*	°C	Calibrated
Morphology – Sink Formation			
a_{Stl}	*Linear coefficient in the stool elongation rate*	mm d^{-1}	Calibrated
$a_{Stl/H}$	*Linear coefficient in the linear relationship Stem height-Stool weight*	m g^{-1}	Calibrated
b_{Rt}	*Root elongation rate*	m d^{-1} °C^{-1}	Calibrated
b_{Stl}	*Constant coefficient in the stool elongation rate*	mm d^{-1} °C^{-1}	Calibrated
$b_{Stl/H}$	*Constant coefficient in the linear relationship Stem height-Stool weight*	m	Calibrated
C_{BtoBr}	*Maximum relative rate of buds producing branches*	d^{-1}	Calibrated
c_{LER}	*Leaf extension, constant*	m	(Porter *et al*., 1993)
f_{fill}	*Power for stem filling rate*	-	Calibrated
$ff_{maxBtoBr}$	*Maximum proportion of buds that produce new branches*	-	Calibrated
h_{0DH}	*Relationship diameter/height intersect*	mm	Measured
LAI_{CShade}	*Minimum LAI for shading to cause senescence*	m^2 m^{-2}	Calibrated
l_{distr}	*Leaf layers distribution*	-	(Cerasuolo *et al*., 2013)
L_{fShp}	*Leaf shape factor*	-	Measured
L_{fWth}	*Leaf width*	m	Measured
ls_{Br}	*Relative reduction of branching with increased LAI*	-	Calibrated
m_{DH}	*Relationship diameter/height slope*	mm m^{-1}	Measured
m_{LER}	*Leaf elongation linear coefficient*	m d^{-1}	(Porter *et al*., 1993)
m_{SER}	*Stem elongation rate, slope*	m d^{-1}	Measured
NL_{Br}	*Number of leaves per branch*	-	Calibrated
n_{Stlwt}	*Power coefficient for the estimation of the stool weight factor*	-	Calibrated
$n_{maxStlwt}$	*Stool weight at which the stool weight factor reaches its maximum effect*	g m^{-2}	Calibrated
ρ_{AG}	*Fraction of assimilates going to the above-ground organs*	-	Measured
ρ_{Rt}	*Fraction of below-ground assimilates going to roots*	-	Measured
ρ_{St}	*Specific stem weight*	g m^{-2}	Measured
SLA_{max}	*Maximum specific leaf area*	m^2 g^{-1}	Measured
SLA_{min}	*Minimum specific leaf area*	m^2 g^{-1}	Measured
St_{max}	*Max stem number given the initial number of buds*	-	Calibrated

η_{St}	*Stems shape parameter*	-	Assumed
Symbol	Definition	Units	Reference/Source
Cont'd Morphology – Sink Formation			
μ_{Br}	*Porter mortality factor - lower asymptote*	-	(Porter *et al*., 1993)
μ_W	*Branches and stems aging death rate*	d^{-1}	Measured
μ_{WRes}	*Percentage of woody reserves lost during the harvest*	$g\ g^{-1}$	Calibrated
σ_{Rt}	*Root dry matter per unit length*	$g\ m^{-1}$	Calibrated
σ_{Stl}	*Stool structural dry matter per unit length*	$g\ m^{-1}$	Calibrated
W_{loss}	*Percentage of dry matter lost during the harvest*	-	Calibrated
Physiology – Source Formation			
Light Interception			
α	*ELADP quadratic coefficient*	-	Observed
β	*ELADP linear coefficient*	-	Observed
γ	*ELADP constant*	-	Observed
η	*Shape parameter for the vertical leaf area distribution*	-	(Cerasuolo *et al*., 2013)
Ω	*Clumping index*	-	Cerasuolo et al. (2013)
μ_T	*Temperature-driven increase of senescence*	d^{-1}	
$\mu_{maxShade}$	*Maximum shading-induced senescence rate*	d^{-1}	Calibrated
μ_{Shade}	*Shading-induced increase of senescence rate per unit of LAI*	d^{-1}	Calibrated
μ_{WS}	*Water stress-driven increase of senescence*	d^{-1}	Calibrated
Assimilation and respiration			
A_{max}	*CO_2 potential assimilation rate at light saturation*	$g(CO_2)\ m^{-2}\ s^{-1}$	(Bonneau, 2004)
P_{cmax}	*Max photosynthetic rate capacity*	$\mu g(CO_2)\ m^{-2}\ s^{-1}$	(Bonneau, 2004)
p_{Lf}	*Percentage of single leaves produced by new flushing buds*	-	Calibrated
Q_{10}	*Responsiveness of respiration at a temperature of 10°C*	-	(Sampson and Ceulemans, 2000)
r_b	*Boundary layer resistance*	$s\ m^{-1}$	Calibrated
R_{BG}	*Maintenance respiration rate of roots*	$g(glucose)\ d^{-1}$	(Vivin *et al*., 2002)
R_D	*Dark respiration*	$\mu g(CO_2)\ m^{-2}\ s^{-1}$	(Kaipiainen, 2009)
Res_{max}	*Maximum Reserve Fraction*	-	Calibrated
Res_{maxStl}	*Maximum reserve fraction of stool DM*	-	Calibrated
R_{Lf}	*Maintenance respiration rate of leaves*	$g(glucose)\ d^{-1}$	Vivin et al. (2002)
$r_{s,min}$	*Minimum stomatal resistance*	$s\ m^{-1}$	Bonneau (2004)
R_{St}	*Maintenance respiration rate of stems*	$g(glucose)\ d^{-1}$	Vivin et al. (2002)
T_{bC}	*Base temperature in CO_2 assimilation*	°C	Assumed
T_{BG}	*Base temperature for below ground growth*	°C	Assumed
T_{maxC}	*Maximum temperature in CO_2 assimilation*	°C	(van Laar *et al*., 1992)
T_{minC}	*Minimum temperature in CO_2 assimilation*	°C	
T_{optC}	*Optimal temperature in CO_2 assimilation*	°C	
WSP	*Water stress parameter*	-	Calibrated
Γ	*CO_2 compensation point at 25°C*	μmol/mole	(Xu *et al*., 2008)
ξ_{GW}	*Conversion of assimilates to biomass*	$g(glucose)\ g^{-1}$	(Penning de Vries *et al*., 1983)
φ_{pot}	*Quantum efficiency of photosynthesis*	$\mu g\ CO_2\ J^{-1}$	Bonneau (2004)
σ	*Scattering coefficient of leaves for PAR*	-	(Goudriaan, 1988)

Table 3: Goodness of fit for modelling growth indicators (LAI, canopy height h_c; number of stems n_{stems}; biomass of stem B_{stem} and stool B_{stool}) and overall yield of four willow varieties grown at Rothamsted for the first (R1, 2010-2011) and second (R2, 2012-2013) rotation used for validation; Residual Mean Square Error (RMSE), Mean Difference (MD), modelling efficiency (ME) and certainty (R^2)

Variety	Indicator	RMSE		MD (O-S)		ME		R^2	
		R1	R2	R1	R2	R1	R2	R1	R2
Endurance	LAI [m^2 m^{-2}]	0.95	1.78	-0.09	-1.24	0.07	-0.45	0.25	0.38
	h_c [m]	0.30	0.26	-0.18	-0.08	0.89	0.96	0.95	0.97
	n_{stems} [m^{-2}]	6.39	7.24	4.40	2.97	0.02	0.15	0.55	0.95
	B_{stem} [Mg ha^{-1}]	1.98	0.87	1.49	0.39	0.90	0.99	0.96	1.00
	B_{stool} [Mg ha^{-1}]	1.37	2.38	0.85	1.74	-0.03	-0.06	0.62	0.58
Resolution	LAI [m^2 m^{-2}]	0.70	0.93	0.45	-0.40	-2.67	-0.23	0.03	0.37
	h_c [m]	0.29	0.32	0.16	-0.18	0.94	0.94	0.96	0.96
	n_{stems} [m^{-2}]	6.64	4.04	3.92	2.04	-0.18	-0.15	0.78	0.66
	B_{stem} [Mg ha^{-1}]	1.86	1.20	0.39	-0.91	0.89	0.99	0.90	1.00
	B_{stool} [Mg ha^{-1}]	0.80	1.57	0.53	1.19	-0.10	-0.01	0.84	0.95
Terra Nova	LAI [m^2 m^{-2}]	0.79	1.17	0.35	-0.63	-0.96	-1.07	0.03	0.35
	h_c [m]	0.23	0.31	0.14	0.16	0.94	0.93	0.96	0.96
	n_{stems} [m^{-2}]	3.87	2.58	-0.19	1.18	0.30	0.11	0.74	0.46
	B_{stem} [Mg ha^{-1}]	1.73	0.99	-0.36	0.22	0.91	0.99	0.95	0.99
	B_{stool} [Mg ha^{-1}]	1.02	1.30	-0.74	-1.29	-0.02	-0.06	0.94	1.00
Tora	LAI [m^2 m^{-2}]	0.45	1.17	0.10	-0.61	-0.63	-1.54	0.15	0.28
	h_c [m]	0.16	0.21	-0.03	0.03	0.97	0.98	0.98	0.98
	n_{stems} [m^{-2}]	2.28	5.15	0.43	4.21	0.44	-1.45	0.76	0.76
	B_{stem} [Mg ha^{-1}]	1.69	0.11	0.04	0.11	0.85	1.00	0.95	1.00
	B_{stool} [Mg ha^{-1}]	0.64	0.96	-0.52	0.49	-0.33	0.56	0.91	0.91
All*	B_{stem} [Mg ha^{-1}]	1.81	0.89	0.38	-0.05	0.90	0.99	0.92	0.99
	B_{stool} [Mg ha^{-1}]	1.00	1.64	0.06	0.53	0.22	0.28	0.26	0.41

*Due to a small number of observations during R2 for biomass (n = 3 compared to >10 for the other indicators), the data were pooled together to have an overall estimation.

Figure captions

Figure 1: Flowchart of the process-based willow growth model, LUCASS, embedded into a water and energy balance framework

Figure 2: Heat map for the average of response strength (μ) estimated using the Morris' method and ranking calculated for all varieties together or separated according to potential and water-limited conditions (All WS&NWS, All NWS, All WS). Average sensitivity was calculated under water-limited conditions for first (WS R1), second rotation (WS R2) separately, for sites considering both rotations (ABER WS R1+R2, ROTH WS R1+R2), and across similar canopy phenotypes (Endurance and Terra Nova – END & TN; Resolution and Tora – RES & T). – Colour intensity increases with increasing response strength but is lower for higher ranks

Figure 3: Morris sensitivity measures (μ*, σ) under water-limited production to random changes of 34 model parameters averaged across all genotypes for Rothamsted (A, C) and Aberystwyth (B, D) during first and second rotation, respectively. Symbols represent pheno- (▪), morpho-(▫) logical sink-related parameters, physiological (•) and other source-related parameters (°)

Figure 4: Observed (filled circles) and simulated (solid line) leaf area index (LAI), canopy height, stem number and accumulated stem (AGB) and stool (BGB) yield of Endurance (A-E) and Tora (F-J) grown at Rothamsted over two consecutive rotations (2010-11; 2012-13). The error bars represent the standard deviations of the experimental values (n=4)

Figure 5: Light use efficiency (LUE, g AGB MJ^{-1} APAR) (A) during the time course of the experiment (2010-2013) for the varieties Tora (□■) and Endurance (Δ▲) at ROTH (open) and ABER (closed) and (B) averaged for all varieties at both sites

Figure 6: Correlations between stem diameter and stem height for Endurance at (A) ROTH and (B) ABER and (C) sketched for all willow varieties (Endurance —, Resolution - - - , Terra Nova — ·· —, Tora ·····) for ROTH (bold) and ABER (fine)

Figure 7: Observed (black) and simulated (white) accumulated yields of four willow varieties (A) for calibration during 1st coppice cycle (2010-2011) at ABER and (B) validation over two 2-year coppice cycles 2010-2011 (a) and 2012-2014 (b) at ROTH

Figure 8: Correlation between measured vs simulated biomass yield of three willow varieties from trials at ROTH (closed symbols) and LARS (open symbols). Endurance : □■, Resolution :Δ▲, Tora: ○●

References

Agostini F, Gregory AS, Richter GM. 2015. Carbon sequestration under perennial energy crops: is the jury still out? *BioEnergy Research* **8**, 000-000.

Amichev BY, Hangs RD, Van Rees KCJ. 2011. A novel approach to simulate growth of multi-stem willow in bioenergy production systems with a simple process-based model (3PG). *Biomass and Bioenergy* **35**, 473-488.

Andralojc PJ, Bencze S, Madgwick PJ, Philippe H, Powers SJ, Shield I, Karp A, Parry MAJ. 2014. Photosynthesis and growth in diverse willow genotypes. *Food and Energy Security* **3**, 69-85.

Aylott MJ, Casella E, Tubby I, Street NR, Smith P, Taylor G. 2008. Yield and spatial supply of bioenergy poplar and willow short-rotation coppice in the UK. *New Phytologist* **178**, 358-370.

Bonneau LJG. 2004. Drought resistance of willow short rotation coppice genotypes. Doctor of Philosophy, Cranfield, Silsoe, 211 + VII.

Bullard MJ, Mustill SJ, Carver P, Nixon PMI. 2002a. Yield improvements through modification of planting density and harvest frequency in short rotation coppice Salix spp. - 2. Resource capture and used in two morphologically diverse varieties. *Biomass & Bioenergy* **22**, 27-39.

Bullard MJ, Mustill SJ, McMillan SD, Nixon PMI, Carver P, Britt CP. 2002b. Yield improvements through modification of planting density and harvest frequency in short rotation coppice Salix spp. - 1. Yield response in two morphologically diverse varieties. *Biomass & Bioenergy* **22**, 15-25.

Cannell MGR, Smith RI. 1983. THERMAL TIME, CHILL DAYS AND PREDICTION OF BUDBURST IN PICEA-SITCHENSIS. *Journal of Applied Ecology* **20**, 951-963.

Cerasuolo M, Richter GM, Cunniff J, Purdy S, Shield I, Karp A. 2013. A pseudo-3D model to optimise the target traits of light interception in short-rotation coppice willow. *Agricultural and Forest Meteorology* **173**, 127-138.

Cesaraccio C, Spano D, Snyder RL, Duce P. 2004. Chilling and forcing model to predict bud-burst of crop and forest species. *Agricultural and Forest Meteorology* **126**, 1-13.

Ceulemans R, McDonald AJS, Pereira JS. 1996. A comparison among eucalypt, poplar and willow characteristics with particular reference to a coppice, growth-modelling approach. *Biomass & Bioenergy* **11**, 215-231.

Chuine I. 2000. A unified model for budburst of trees. *Journal of Theoretical Biology* **207**, 337-347.

Cunniff J, Purdy SJ, Barraclough T, Castle M, Maddison AL, Jones LE, Shield IF, Gregory AS, Karp A. 2015. High yielding biomass ideotypes of willow (Salix spp.) show differences in below ground biomass allocation. *Biomass & Bioenergy* **80**, 114-127.

Cunniff J, Shield I, Barraclough T, Castle M, Hanley S, Andralojc J, Richter G, Cerasuolo M, Purdy S, Clifton-Brown J, Maddison A, Jones L, Donnison I, Karp A. 2011. BSBEC-BioMASS - Selecting traits to optimise biomass yield of SRC willow. *Biomass and Energy Crops*, Vol. Aspects of Applied Biology, 83-91.

Cunniff J, Shield I, Purdy S, Karp A. 2014. Phenological dynamics of above and below ground biomass and non- structural carbohydrates in the perennial bioenergy crop willow. International Poplar Symposium.

de Neergaard A, Porter JR, Gorissen A. 2002. Distribution of assimilated carbon in plants and rhizosphere soil of basket willow (Salix viminalis L.). *Plant and Soil* **245**, 307-314.

De Pury DGG, Farquhar GD. 1997. Simple scaling of photosynthesis from leaves to canopies without the errors of big-leaf models. *Plant, Cell and Environment* **20**, 537-557.

Deckmyn G, Laureysens I, Garcia J, Muys B, Ceulemans R. 2004. Poplar growth and yield in short rotation coppice: model simulations using the process model SECRETS. *Biomass & Bioenergy* **26**, 221-227.
Deckmyn G, Verbeeck H, de Beeck MO, Vansteenkiste D, Steppe K, Ceulemans R. 2008. ANAFORE: A stand-scale process-based forest model that includes wood tissue development and labile carbon storage in trees. *Ecological Modelling* **215**, 345-368.
Fourcaud T, Zhang X, Stokes A, Lambers H, Korner C. 2008. Plant growth modelling and applications: The increasing importance of plant architecture in growth models. *Annals of Botany* **101**, 1053-1063.
Fracheboud Y, Luquez V, Bjorken L, Sjodin A, Tuominen H, Jansson S. 2009. The Control of Autumn Senescence in European Aspen. *Plant Physiology* **149**, 1982-1991.
Fu YH, Campioli M, Deckmyn G, Janssens IA. 2013. Sensitivity of leaf unfolding to experimental warming in three temperate tree species. *Agricultural and Forest Meteorology* **181**, 125-132.
Fu YS, Campioli M, Van Oijen M, Deckmyn G, Janssens IA. 2012. Bayesian comparison of six different temperature-based budburst models for four temperate tree species. *Ecological Modelling* **230**, 92-100.
Genard M, Dauzat J, Franck N, Lescourret F, Moitrier N, Vaast P, Vercambre G. 2008. Carbon allocation in fruit trees: from theory to modelling. *Trees-Structure and Function* **22**, 269-282.
Goudriaan J. 1988. The Bare Bones of Leaf-Angle Distribution in Radiation Models for Canopy Photosynthesis and Energy Exchange. *Agricultural and Forest Meteorology* **43**, 155-169.
Goudriaan J, van Laar HH. 1994. *Modelling Potential Crop Growth Processes. Textbook with Exercises*. Wageningen: Kluwer Academic Publishers.
Guidi W, Tozzini C, Bonari E. 2009. Estimation of chemical traits in poplar short-rotation coppice at stand level. *Biomass & Bioenergy* **33**, 1703-1709.
Heilman PE, Ekuan G, Fogle D. 1994. ABOVEGROUND AND BELOWGROUND BIOMASS AND FINE ROOTS OF 4-YEAR-OLD HYBRIDS OF POPULUS-TRICHOCARPA X POPULUS-DELTOIDES AND PARENTAL SPECIES IN SHORT-ROTATION CULTURE. *Canadian Journal of Forest Research-Revue Canadienne De Recherche Forestiere* **24**, 1186-1192.
Hlaszny E, Hajdu E, Gy B, Ladanyi M. 2012. COMPARISON OF BUDBURST MODELS PREDICTIONS FOR KEKFRANKOS. *Applied Ecology and Environmental Research* **10**, 75-86.
Hoeglind M, Hanslin HM, Van Oijen M. 2005. Timothy regrowth, tillering and leaf area dynamics following spring harvest at two growth stages. *Field Crops Research* **93**, 51-63.
Horvath DP, Anderson JV, Chao WS, Foley ME. 2003. Knowing when to grow: signals regulating bud dormancy. *Trends in Plant Science* **8**, 534-540.
Jing Q, Conijn SJG, Jongschaap REE, Bindraban PS. 2012. Modeling the productivity of energy crops in different agro-ecological environments. *Biomass and Bioenergy* **46**, 618-633.
Kaipiainen E. 2009. Parameters of photosynthesis light curve in *Salix dasyclados* and their changes during the growth season. *Russian Journal of Plant Physiology* **56**, 445-453.
Karp A, Hanley SJ, Trybush SO, Macalpine W, Pei M, Shield I. 2011. Genetic Improvement of Willow for Bioenergy and BiofuelsFree Access. *Journal of Integrative Plant Biology* **53**, 151-165.
Karp A, Richter GM, Shield IF, Hanley SH. 2014. Genetics, genomics and crop modelling: integrative approaches to the improvement of biomass willows. In: McCann MC, Buckeridge MS, Carpita NC, eds. *Plants and BioEnergy*, Vol. 4. New York: Springer Science+Business Media, 107-130.
Karp A, Shield I. 2008. Bioenergy from plants and the sustainable yield challenge. *New Phytologist* **179**, 15-32.

Kauter D, Lewandowski I, Claupein W. 2003. Quantity and quality of harvestable biomass from Populus short rotation coppice for solid fuel use--a review of the physiological basis and management influences. *Biomass and Bioenergy* **24**, 411-427.
Larsen S, Jørgensen U, Lærke P. 2014. Willow Yield Is Highly Dependent on Clone and Site. *BioEnergy Research* **7**, 1280-1292.
Larsson S. 1998. Genetic improvement of willow for short-rotation coppice. *Biomass and Bioenergy* **15**, 23-26.
Laureysens I, Deraedt W, Indeherberge T, Ceulemans R. 2003. Population dynamics in a 6-year old coppice culture of poplar. I. Clonal differences in stool mortality, shoot dynamics and shoot diameter distribution in relation to biomass production. *Biomass and Bioenergy* **24**, 81-95.
Le Roux X, Lacointe A, Escobar-Gutierrez A, Le Dizes S. 2001. Carbon-based models of individual tree growth: A critical appraisal. *Annals of Forest Science* **58**, 469-506.
Martin PJ, Stephens W. 2006. Willow growth in response to nutrients and moisture on a clay landfill cap soil. I. Growth and biomass production. *Bioresource Technology* **97**, 437-448.
Martin PJ, Stephens W. 2008. Willow water uptake and shoot extension growth in response to nutrient and moisture on a clay landfill cap soil. *Bioresource Technology* **99**, 5839-5850.
Matthews RW. 2001. Modelling of energy and carbon budgets of wood fuel coppice systems. *Biomass & Bioenergy* **21**, 1-19.
Mcdonald AJS, Stadenberg I. 1993. Diurnal Pattern of Leaf Extension in Salix-Viminalis Relates to the Difference in Leaf Turgor before and after Stress-Relaxation. *Tree Physiology* **13**, 311-318.
Morin X, Ameglio T, Ahas R, Kurz-Besson C, Lanta V, Lebourgeois F, Miglietta F, Chuine I. 2007. Variation in cold hardiness and carbohydrate concentration from dormancy induction to bud burst among provenances of three European oak species. *Tree Physiology* **27**, 817-825.
Morris MD. 1991. Factorial sampling plans for preliminary computational experiments. *Technometrics* **33**, 161-174.
Pacaldo RS, Volk TA, Briggs RD. 2013. Greenhouse Gas Potentials of Shrub Willow Biomass Crops Based on Below- and Aboveground Biomass Inventory Along a 19-Year Chronosequence. *BioEnergy Research* **6**, 252-262.
Payne RW, Harding SA, Murray DA, Soutar DM, Baird DB, Glaser AI, Welham SJ, Gilmour AR, Thompson R, Webster R. 2011. *The Guide to GenStat Release 14*. Hemel Hempstead, UK: VSN International.
Penning de Vries FWT, Van Laar HH, Chardon MCM. 1983. Bioenergetics of growth of seeds, fruits and storage organs. In: Smith WH, Banta SJ, eds. *Potential productivity of field crops under different environments*. Los Banos, Philippines:: IRRI, 37-59.
Perttu KL, Philippot S. 1996. Modelling short rotation forestry growth (Uppsala, Sweden, 24-26 October 1994). *Biomass & Bioenergy* **11**, 69-71.
Philippot S. 1996. Simulation models of short-rotation forestry production and coppice biology. *Biomass & Bioenergy* **11**, 85-93.
Porter JR, Parfitt RI, Arnold GM. 1993. Leaf Demography in Willow Short-Rotation Coppice. *Biomass & Bioenergy* **5**, 325-336.
Powers SJ, Peacock L, Yap ML, Brain P. 2006. Simulated beetle defoliation on willow genotypes in mixture and monotype plantations. *Annals of Applied Biology* **148**, 27-38.
Pretzsch H, Grote R, Reineking B, Roetzer T, Seifert S. 2008. Models for forest ecosystem management: A European perspective. *Annals of Botany* **101**, 1065-1087.
Richter GM, Acutis M, Trevisiol P, Latiri K, Confalonieri R. 2010. Sensitivity analysis for a complex crop model applied to Durum wheat in the Mediterranean. *European Journal of Agronomy* **32**, 127-136.
Richter GM, Rana G, Ferrara RM, Ventrella D, Acutis M, Trevisiol P, Mayr T, Baggaley N, Morris J, Holmes A, Trawick P, Dailey AG, Robbins P, Simota C,

Whitmore AP, Powlson DS. 2006. Stability and Mitigation of Arable Systems in Hilly Landscapes. *Final Report*. Brussels: European Commission, 280.
Rinne PLH, Welling A, Vahala J, Ripel L, Ruonala R, Kangasjarvi J, van der Schoot C. 2011. Chilling of Dormant Buds Hyperinduces FLOWERING LOCUS T and Recruits GA-Inducible 1,3-beta-Glucanases to Reopen Signal Conduits and Release Dormancy in Populus. *Plant Cell* **23**, 130-146.
Robinson KM, Karp A, Taylor G. 2004. Defining leaf traits linked to yield in short-rotation coppice Salix. *Biomass & Bioenergy* **26**, 417-431.
Rohde A, Bhalerao RP. 2007. Plant dormancy in the perennial context. *Trends in Plant Science* **12**, 217-223.
Rytter RM. 2001. Biomass production and allocation, including fine-root turnover, and annual N uptake in lysimeter-grown basket willows. *Forest Ecology and Management* **140**, 177-192.
Sampson DA, Ceulemans R. 2000. SECRETS: simulated carbon fluxes from a mixed coniferous/deciduous Belgian forest. In: Ceulemans R, Veroustraete F, Gond V, Van Rensbergen JBHF, eds. *Forest ecosystem modeling, upscaling and remote sensing*: SPB Academic Publishing bv, 95 -108.
Sannervik AN, Eckersten H, Verwijst T, Kowalik P, Nordh N-E. 2006. Simulation of willow productivity based on radiation use efficiency, shoot mortality and shoot age. *European Journal of Agronomy* **24**, 156-164.
Savage JA, Cavender-Bares J, Verhoeven A. 2009. Willow species (genus: Salix) with contrasting habitat affinities differ in their photoprotective responses to water stress. *Functional Plant Biology* **36**, 300-309.
Savage JA, Cavender-Bares JM. 2011. Contrasting drought survival strategies of sympatric willows (genus: Salix): consequences for coexistence and habitat specialization. *Tree Physiology* **31**, 604-614.
Schapendonk AHCM, Stol W, van Kraalingen DWG, Bouman BAM. 1998. LINGRA, a sink/source model to simulate grassland productivity in Europe. *European Journal of Agronomy* **9**, 87-100.
Sennerby-Forsse L, Zsuffa L. 1995. Bud structure and resprouting in coppiced stools of *Salix viminalis* L., *S. eriocephal*a; Michx., and *S. amygdaloides* Anders. *Trees - Structure and Function* **9**, 224-234.
Sinclair TR. 1986. Water and nitrogen limitations in soybean grain production. Part I. Model development. *Field Crops Res.* **15**, 125 – 141.
Smith P, Smith JU, Powlson DS, McGill WB, Arah JRM, Chertov OG, Coleman K, Franko U, Frolking S, Jenkinson DS, Jensen LS, Kelly RH, Klein-Gunnewiek H, Komarov AS, Li C, Molina JAE, Mueller T, Parton WJ, Thornley JHM, Whitmore AP. 1997. A comparison of the performance of nine soil organic matter models using datasets from seven long-term experiments. *Geoderma* **81**, 153-225.
Stanton BJ, Serapiglia MJ, Smart LB. 2014. The domestication and conservation of Populus and Salix genetic resources. In: Isebrands JG, Richardson J, eds. *Poplars and willows: trees for society and the environment*. Wallingford, UK: CAB International, 124-199.
Tallis MJ, Casella E, Henshall PA, Aylott MJ, Randle TJ, Morison JIL, Taylor G. 2013. Development and evaluation of ForestGrowth-SRC a process-based model for short rotation coppice yield and spatial supply reveals poplar uses water more efficiently than willow. *Global Change Biology Bioenergy* **5**, 53-66.
Teixeira EI, Moot DJ, Brown HE, Pollock KM. 2007. How does defoliation management impact on yield, canopy forming processes and light interception of lucerne (Medicago sativa L.) crops? *European Journal of Agronomy* **27**, 154-164.
Tharakan PJ, Volk TA, Nowak CA, Ofezu GJ. 2008. Assessment of Canopy Structure, Light Interception, and Light-use Efficiency of First Year Regrowth of Shrub Willow (Salix sp.). *BioEnergy Research* **1**, 229-238.

Toillon J, Rollin B, Dalle E, Feinard-Duranceau M, Bastien J-C, Brignolas F, Marron N. 2013. Variability and plasticity of productivity, water-use efficiency, and nitrogen exportation rate in Salix short rotation coppice. *Biomass & Bioenergy* **56**, 392-404.
Tschaplinski TJ, Blake TJ. 1994. Carbohydrate mobilization following shoot defoliation and decapitation in hybrid poplar. *Tree Physiology* **14**, 141-151.
Tschaplinski TJ, Blake TJ. 1995. Growth and carbohydrate status of coppice shoots of hybrid poplar following shoot pruning. *Tree Physiology* **15**, 333-338.
van Laar HH, Goudriaan J, van Keulen H. 1992. Simulation of crop growth for potential and water limited production situations (as applied to spring wheat). In: CABO-TT, ed. *Simulation Reports*, Vol. 27. Wageningen, The Netherlands: CABO-DLO/Theoretical Production Ecology -Wageningen Agricultural University, 78 pp.
Verlinden MS, Broeckx LS, Van den Bulcke J, Van Acker J, Ceulemans R. 2013. Comparative study of biomass determinants of 12 poplar (Populus) genotypes in a high-density short-rotation culture. *Forest Ecology and Management* **307**, 101-111.
Verwijst T, Lundkvist A, Edelfeldt S, Forkman J, Nordh N-E. 2012. Effects of clone and cutting traits on shoot emergence and early growth of willow. *Biomass and Bioenergy* **37**, 257-264.
Vivin PH, Castelan M, Gaudillère JP. 2002. A Source/Sink Model to Simulate Seasonal Allocation of Carbon in grapevine. *Acta Hort. (ISHS)* **584**, 43-56.
Volk TA, Abrahamson LP, Nowak CA, Smart LB, Tharakan PJ, White EH. 2006. The development of short-rotation willow in the northeastern United States for bioenergy and bioproducts, agroforestry and phytoremediation. *Biomass & Bioenergy* **30**, 715-727.
Von Fircks Y, Sennerby-Forsse L. 1998. Seasonal fluctuations of starch in root and stem tissues of coppiced Salix viminalis plants grown under two nitrogen regimes. *Tree Physiology* **18**, 243-249.
Weih M. 2009. Genetic and environmental variation in spring and autumn phenology of biomass willows (Salix spp.): effects on shoot growth and nitrogen economy. *Tree Physiology* **29**, 1479-1490.
Weih M, Nordh NE. 2002. Characterising willows for biomass and phytoremediation: growth, nitrogen and water use of 14 willow clones under different irrigation and fertilisation regimes. *Biomass & Bioenergy* **23**, 397-413.
Weih M, Nordh NE. 2005. Determinants of biomass production in hybrid willows and prediction of field performance from pot studies. *Tree Physiology* **25**, 1197-1206.
Wösten JHM, Lilly A, Nemes A, Le Bas C. 1999. Development and use of a database of hydraulic properties of European soils. *Geoderma* **90**, 169-185.
Xu X, Peng GQ, Wu CC, Korpelainen H, Li CY. 2008. Drought inhibits photosynthetic capacity more in females than in males of Populus cathayana. *Tree Physiology* **28**, 1751-1759.

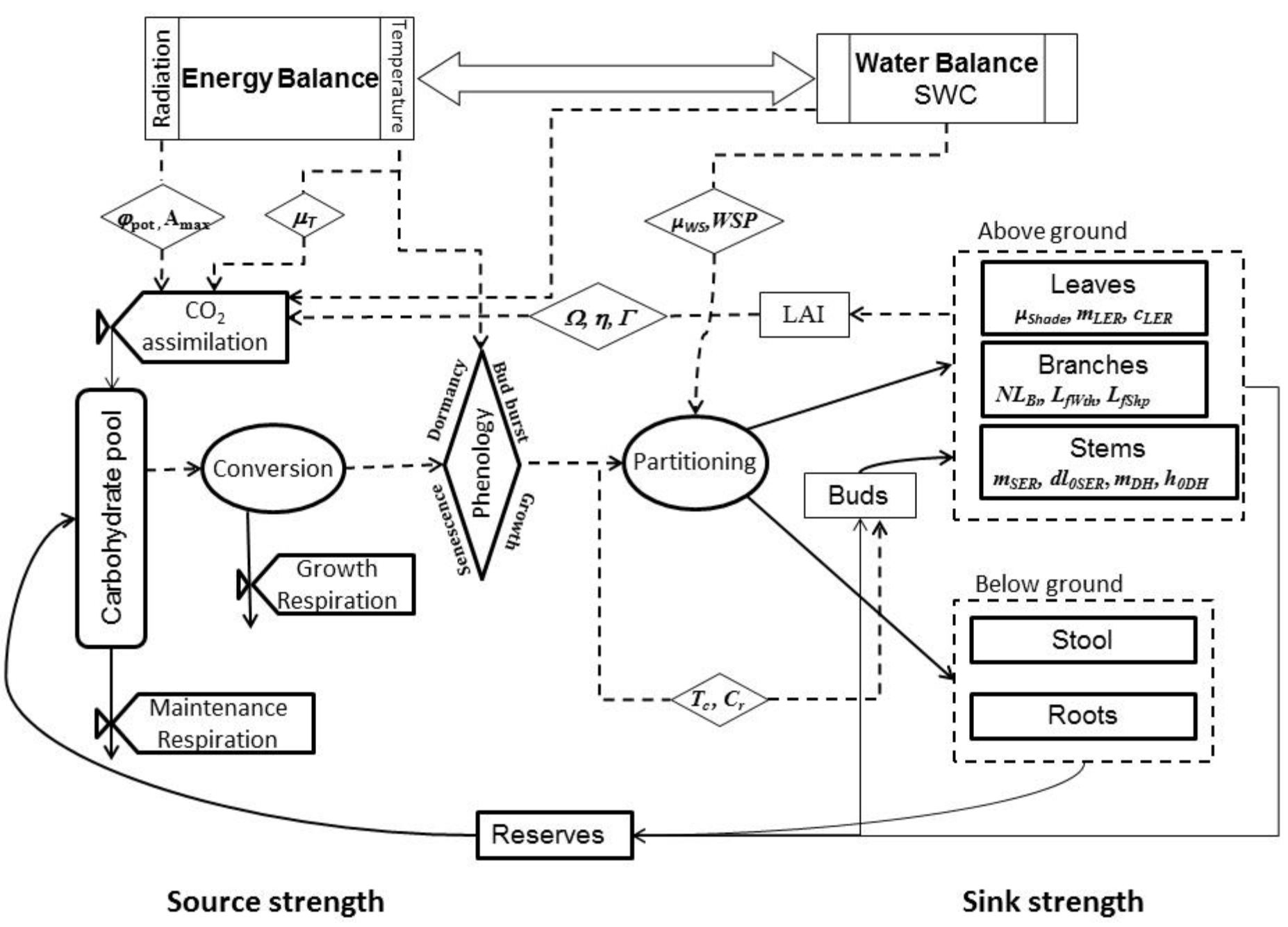
Radiation
Energy Balance
Temperature
Water Balance
SWC
φ_{pot}, A_{max}
μ_T
μ_{WS}, WSP
Above ground
CO_2 assimilation
Ω, η, Γ
LAI
Leaves
μ_{Shade}, m_{LER}, c_{LER}
Branches
NL_B, L_{fWth}, L_{fSkp}
Stems
m_{SER}, dl_{0SER}, m_{DH}, h_{0DH}
Carbohydrate pool
Conversion
Dormancy
Bud burst
Phenology
Senescence
Growth
Partitioning
Buds
Growth Respiration
Below ground
Stool
Roots
Maintenance Respiration
T_c, C_r
Reserves
Source strength
Sink strength

		Average Strength									Rank of strength								
		All WS&NWS	All NWS	All WS	WS R1	WS R2	ABER WS R1+R2	ROTH WS R1+R2	WS END & TN	WS RES & T	All WS&NWS	All NWS	All WS	WS R1	WS R2	ABER WS R1+R2	ROTH WS R1+R2	WS END & TN	WS RES & T
Phenology	C_r	1,535	2451	619	352	886	476	762	782	989	10	9	17	9	19	17	16	21	15
	dl_{BtoBr}	1,866	2967	765	276	1254	355	1176	1344	1165	8	6	13	12	13	22	5	13	12
	dl_{BMax}	1,161	1569	753	104	1402	497	1009	1832	973	15	16	14	24	10	15	10	7	16
	dl_{OSER}	9,184	12083	6285	2441	10129	6641	5929	11941	8317	1	1	1	1	1	1	1	1	1
	f_{fill}	548	876	219	88	351	105	334	449	252	22	20	25	25	25	29	23	24	26
	dd_{fill}	420	539	301	146	456	205	396	588	324	24	22	23	21	23	24	22	23	24
	b_{Rt}	391	0	783	12	1554	765	801	1546	1561	25	34	11	32	9	11	15	11	7
	T_c	686	737	636	173	1098	435	836	1136	1060	20	21	16	19	16	20	14	15	13
Morphology	ρ_{AG}	2,482	4147	816	302	1330	595	1037	1857	803	4	3	10	11	11	13	9	6	18
	h_{0DH}	504	479	529	272	786	451	607	787	785	23	24	20	13	21	18	18	20	19
	c_{LER}	986	1390	581	257	905	570	593	816	995	16	17	19	15	18	14	19	19	14
	m_{LER}	2,011	2669	1354	718	1990	1523	1185	2061	1920	6	8	4	5	4	4	4	5	4
	m_{SER}	2,978	4011	1945	998	2892	1791	2099	3502	2281	2	4	2	3	2	2	3	2	3
	m_{DH}	1,781	2380	1182	751	1614	1248	1117	1788	1439	9	10	6	4	7	6	7	10	8
	NL_{Br}	2,422	3601	1242	498	1986	1331	1153	2062	1910	5	5	5	7	5	5	6	4	5
	$NBuds_0$	658	986	330	257	404	397	264	388	420	21	19	22	16	24	21	25	25	22
	p_{Lf}	1,381	1760	1001	234	1768	1126	876	1790	1746	12	14	7	18	6	7	13	9	6
	ρ_{Rt}	1,425	1900	949	614	1285	946	953	1206	1364	11	12	9	6	12	8	11	14	10
	ff_{max}	844	1089	598	267	930	685	511	1095	765	18	18	18	14	17	12	21	16	21
Light Interception	k_C	45	69	21	8	34	23	19	45	23	34	31	33	33	33	33	33	33	33
	Ω	1,301	2348	254	32	476	177	331	701	250	13	11	24	28	22	26	24	22	27
	LAI_{CShade}	173	345	1	0	2	1	0	3	0	30	25	35	35	35	35	35	35	35
	SLA_{max}	228	336	121	84	159	119	124	203	115	28	26	28	26	30	28	28	28	29
	SLA_{min}	39	50	29	18	39	31	26	46	31	35	32	32	31	32	31	32	32	32
	η	835	1577	94	22	166	71	117	265	68	19	15	30	29	29	30	29	26	30
Physiology	ρ_{20}	208	223	193	110	277	225	162	176	378	29	27	26	23	26	23	27	30	23
	φ_{pot}	2,683	4655	710	254	1166	491	930	1465	867	3	2	15	17	14	16	12	12	17
	A_{max}	1,189	1866	512	168	856	444	580	941	772	14	13	21	20	20	19	20	18	20
	μ_T	1,938	2902	974	342	1607	869	1080	1813	1401	7	7	8	10	8	9	8	8	9
	μ_{Shade}	50	98	2	0	4	3	1	8	0	33	30	34	34	34	34	34	34	34
	μ_{WS}	384	0	767	431	1103	792	743	1001	1206	26	33	12	8	15	10	17	17	11
	$d_{AfterCut}$	363	537	189	144	233	202	175	210	256	27	23	27	22	27	25	26	27	25
	Res_{max}	157	196	118	35	200	139	96	191	210	31	28	29	27	28	27	30	29	28
	μ_W	96	159	34	20	48	25	43	63	33	32	29	31	30	31	32	31	31	31
	WSP	972	0	1944	1128	2760	1706	2182	2400	3120	17	34	3	2	3	3	2	3	2

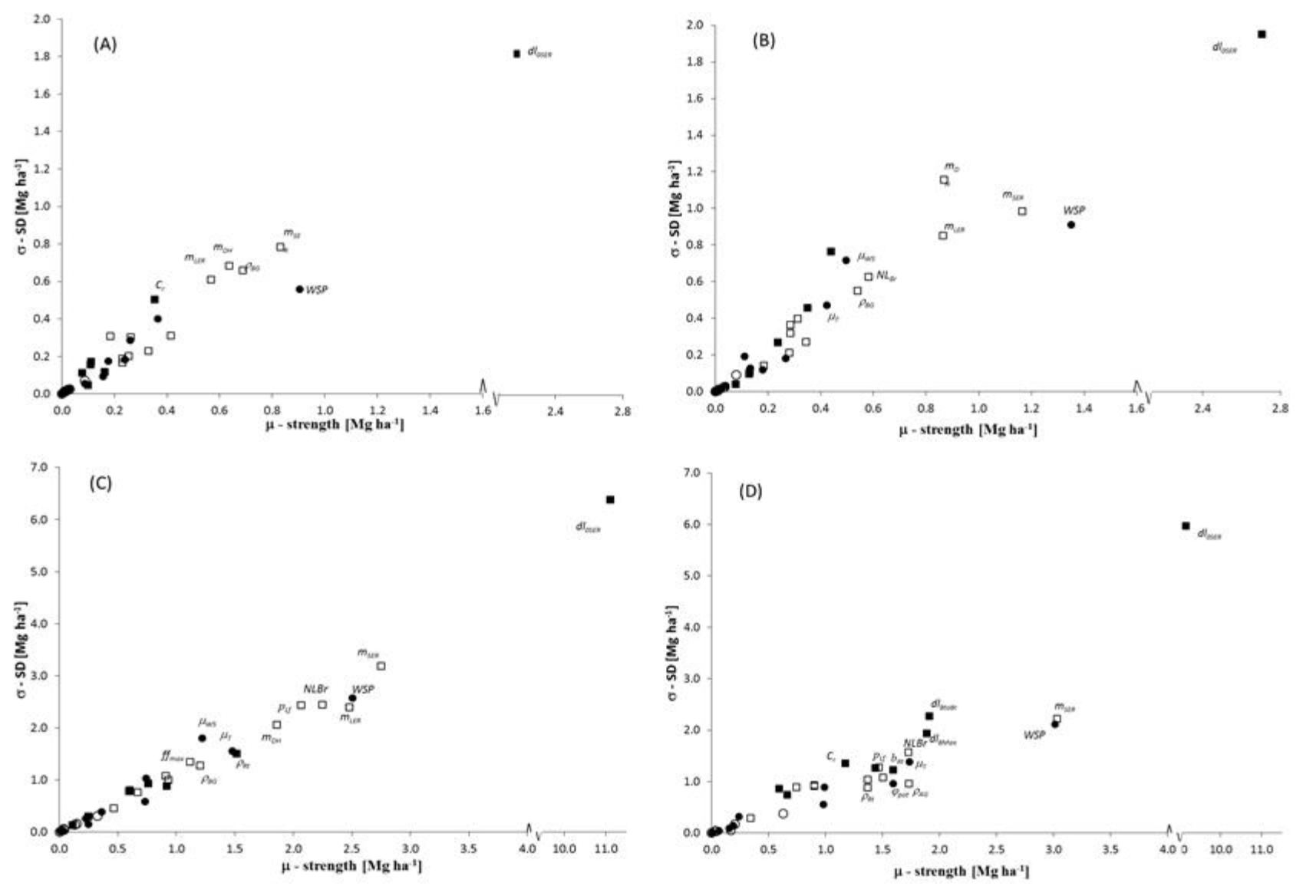
(A)
(B)
(C)
(D)
σ - SD [Mg ha⁻¹]
μ - strength [Mg ha⁻¹]
WSP
NLBr

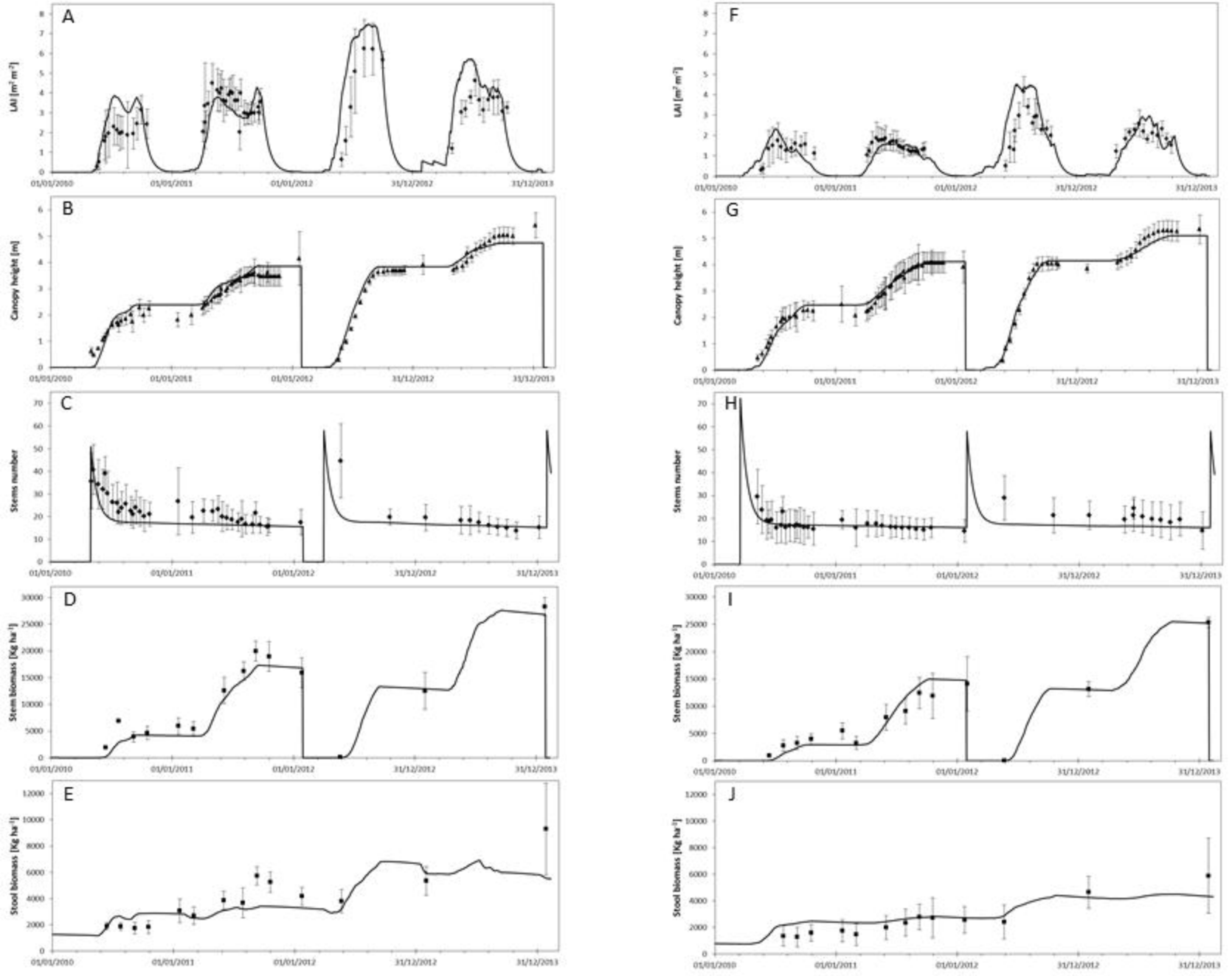
A
LAI [m² m⁻²]
B
Canopy height [m]
C
Stems number
D
Stem biomass [Kg ha⁻¹]
E
Stool biomass [Kg ha⁻¹]
F
LAI [m² m⁻²]
G
Canopy height [m]
H
Stems number
I
Stem biomass [Kg ha⁻¹]
J
Stool biomass [Kg ha⁻¹]
01/01/2010
01/01/2011
01/01/2012
31/12/2012
31/12/2013

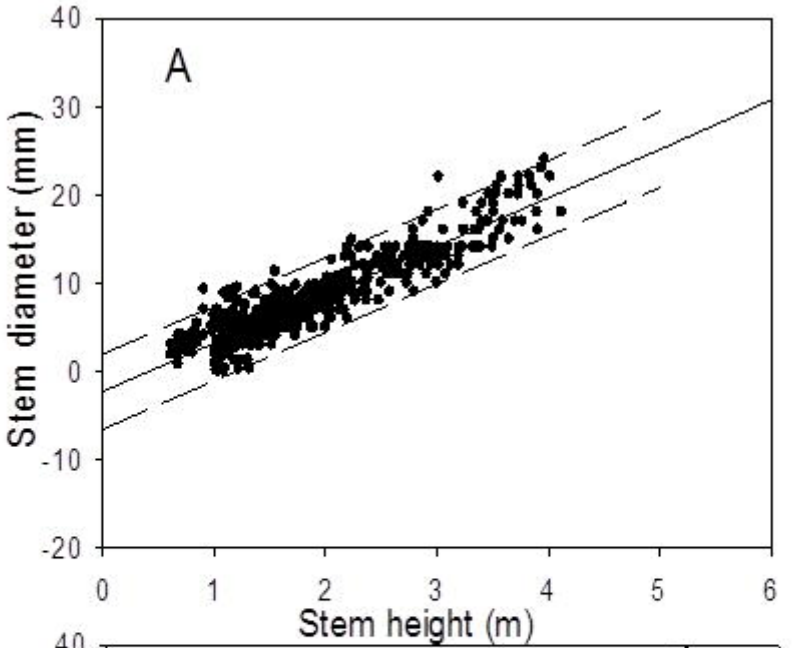
A
Stem diameter (mm)
40
30
20
10
0
-10
-20
0
1
2
3
4
5
6
Stem height (m)

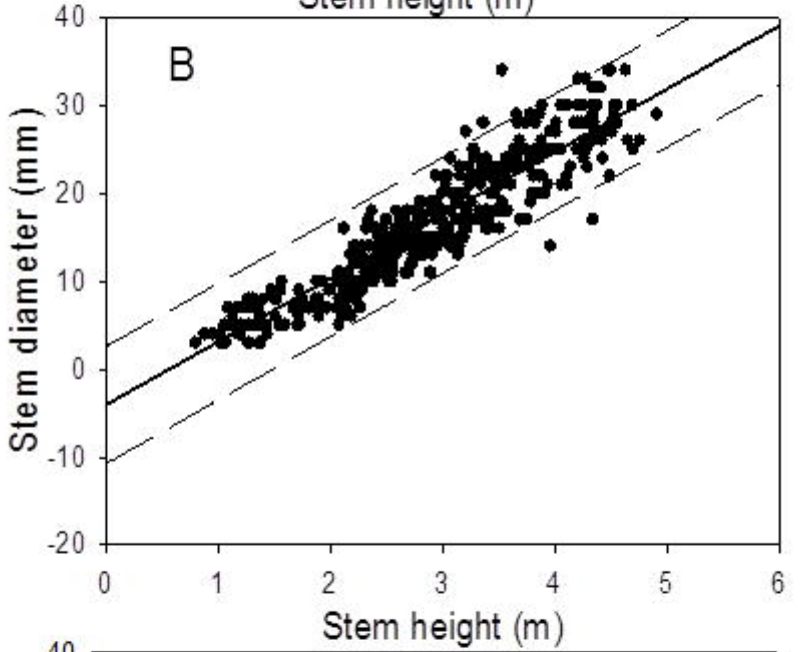
B
Stem diameter (mm)
40
30
20
10
0
-10
-20
0
1
2
3
4
5
6
Stem height (m)

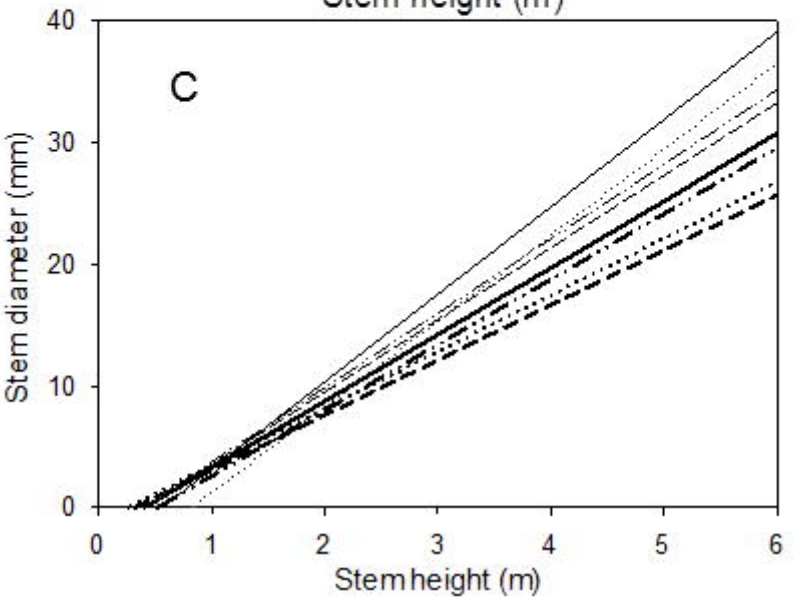
C
Stem diameter (mm)
40
30
20
10
0
0
1
2
3
4
5
6
Stem height (m)

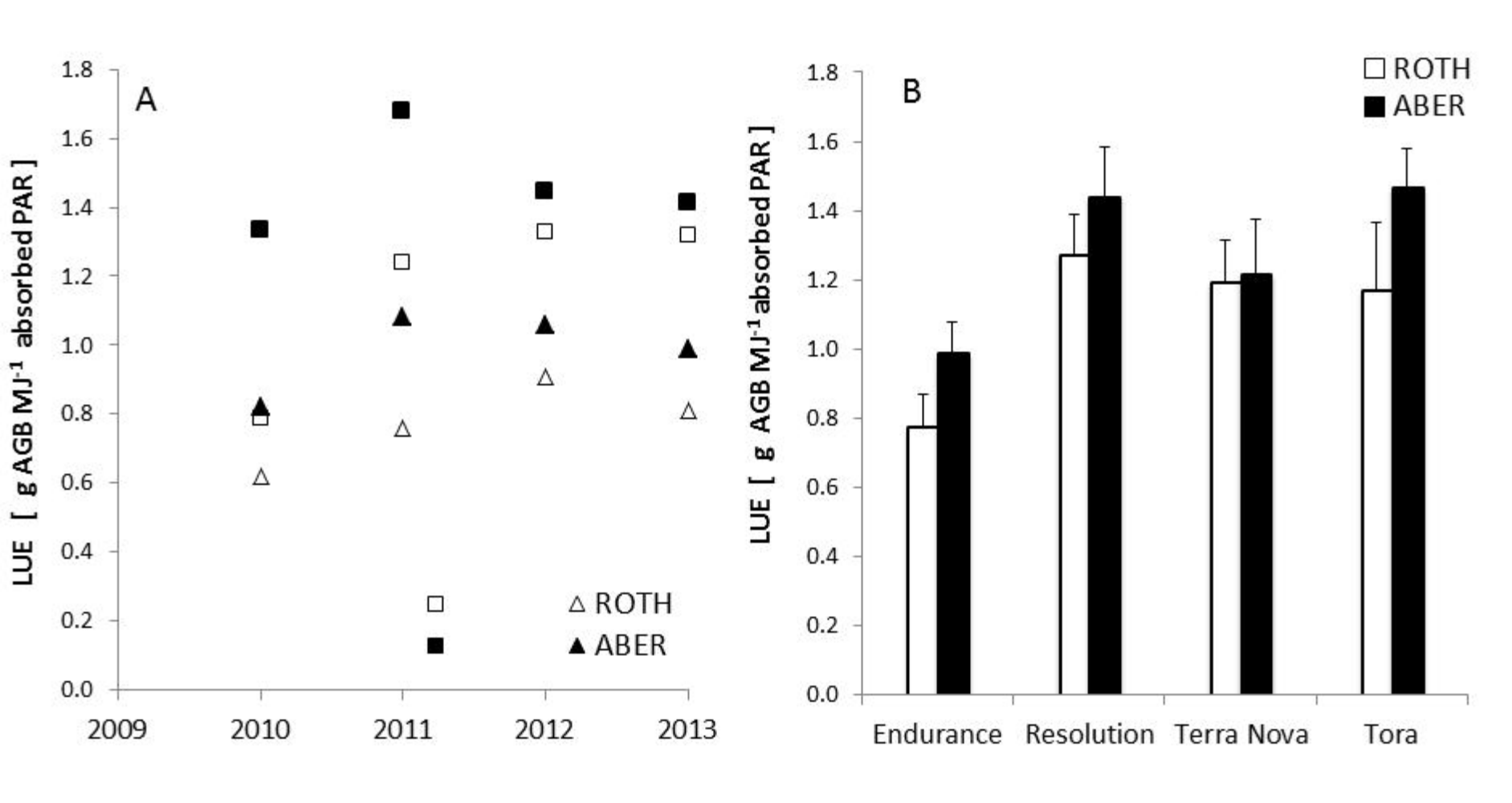
A
B
LUE [g AGB MJ-1 absorbed PAR]
1.8
1.6
1.4
1.2
1.0
0.8
0.6
0.4
0.2
0.0
2009
2010
2011
2012
2013
ROTH
ABER
Endurance
Resolution
Terra Nova
Tora

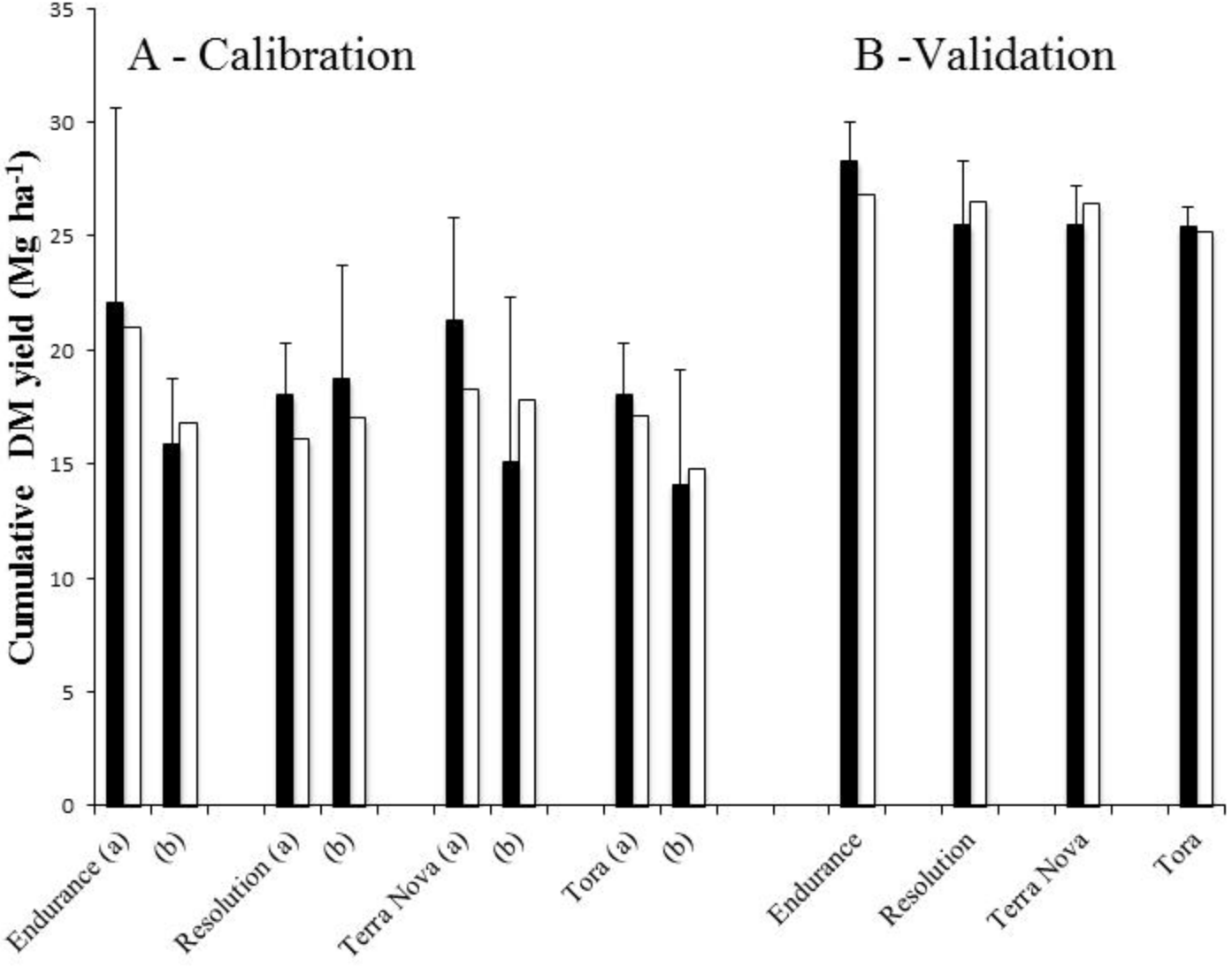
A - Calibration
B -Validation
Cumulative DM yield (Mg ha-1)
35
30
25
20
15
10
5
0
Endurance (a)
(b)
Resolution (a)
(b)
Terra Nova (a)
(b)
Tora (a)
(b)
Endurance
Resolution
Terra Nova
Tora

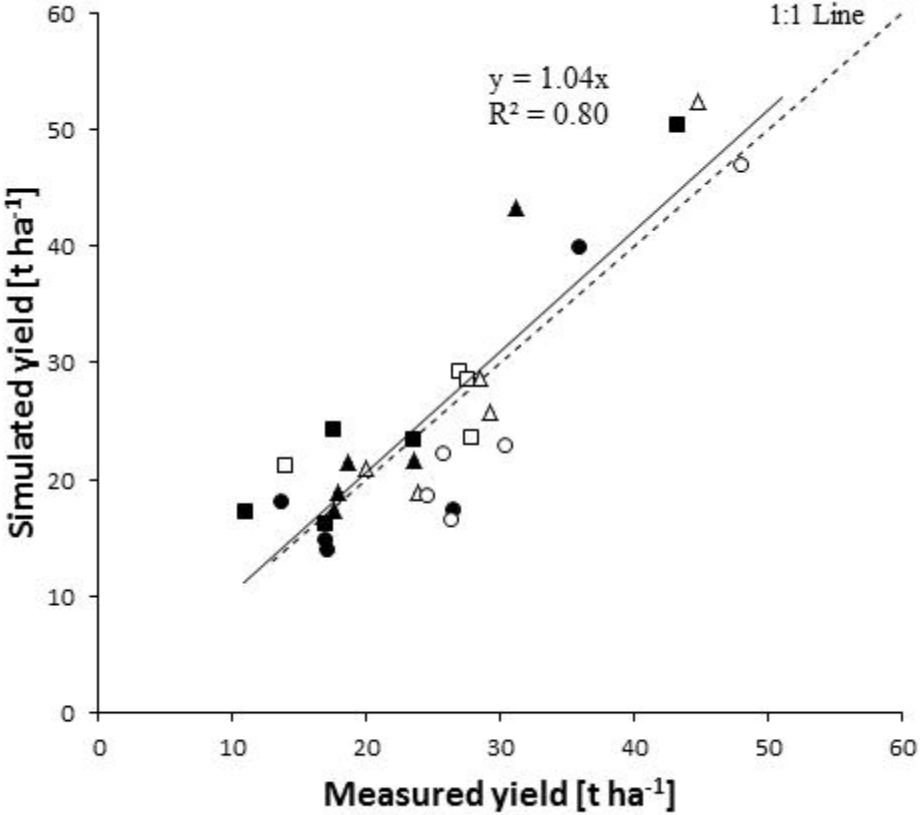
1:1 Line
y = 1.04x
R² = 0.80
Simulated yield [t ha-1]
Measured yield [t ha-1]
0
10
20
30
40
50
60